AMELIORATION OF DUCHENNE MUSCULAR DYSTROPHY IN MDX MICE BY ELIMINATION OF MATRIX-ASSOCIATED FIBRIN-DRIVEN INFLAMMATION COUPLED TO THE $\alpha_M\beta_2$ LEUKOCYTE INTEGRIN RECEPTOR

Berta Vidal[1], Esther Ardite[1], Mònica Suelves[1], Vanessa Ruiz-Bonilla[1], Anna Janué[1], Matthew J. Flick[2], Jay L. Degen[2], Antonio L. Serrano[1] and Pura Muñoz-Cánoves[1,3*]*

[1]Cell Biology Group, Department of Experimental and Health Sciences, Pompeu Fabra University (UPF), CIBER on Neurodegenerative diseases (CIBERNED), Barcelona, Spain; [2] Experimental Hematology, Cincinnati Children's Hospital Medical Center, Cincinnati, Ohio, USA; [3]Institució Catalana de Recerca i Estudis Avançats (ICREA), Barcelona, Spain

* Equal contribution

Corresponding authors:

Pura Muñoz-Cánoves (pura.munoz@upf.edu)
Department of Experimental & Health Sciences
University Pompeu Fabra (UPF)
Dr. Aiguader 88
08003 Barcelona Spain
Tel: +34 933160891
Fax: +34 933160901

Antonio L. Serrano (antonio.serrano@upf.edu)
Department of Experimental & Health Sciences
University Pompeu Fabra (UPF)
Dr. Aiguader 88
08003 Barcelona Spain
Tel: +34 933160889
Fax: +34 933160901

ABSTRACT

In Duchenne Muscular Dystrophy (DMD), a persistently altered and reorganizing extracellular matrix (ECM) within inflamed muscle promotes damage and dysfunction. However, the molecular determinants of the ECM that mediate inflammatory changes and faulty tissue reorganization remain poorly defined. Here, we show that fibrin deposition is a conspicuous consequence of muscle-vascular damage in dystrophic muscles of DMD patients and mdx mice and that elimination of fibrin(ogen) attenuated dystrophy progression in mdx mice. These benefits appear to be tied to: (i) a decrease in leukocyte integrin $\alpha_M\beta_2$-mediated proinflammatory programs, thereby attenuating counterproductive inflammation and muscle degeneration; and (ii) a release of satellite cells from persistent inhibitory signals, thereby promoting regeneration. Remarkably, $Fib\gamma^{390\text{-}396A}$ mice expressing a mutant form of fibrinogen with normal clotting function, but lacking the $\alpha_M\beta_2$ binding motif, ameliorated dystrophic pathology. Delivery of a fibrinogen/$\alpha_M\beta_2$ blocking peptide was similarly beneficial. Conversely, intramuscular fibrinogen delivery sufficed to induce inflammation and degeneration in fibrinogen-null mice. Thus, local fibrin(ogen) deposition drives dystrophic muscle inflammation and dysfunction, and disruption of fibrin(ogen)-$\alpha_M\beta_2$ interactions may provide a novel strategy for DMD treatment.

INTRODUCTION

Duchenne muscular dystrophy (DMD) is one of the most common X-linked lethal diseases, affecting 1 in 3,500 newborn males. DMD results from mutations in the gene coding for the protein dystrophin, a cytoskeletal protein localized at the interface of the actin-based contractile apparatus and the sarcolemma. In the absence of a functional dystrophin complex tethering the actin cytoskeleton inside the muscle cell to the extracellular matrix (ECM), forces generated by the muscle fiber contraction result in muscle fiber damage due to shearing of the sarcolemma (reviewed in 1). The mdx mouse strain, which carries a naturally occurring nonsense mutation in exon 2 resulting in loss of dystrophin protein production, is the most widely used animal model for DMD (2-3). DMD patients and mdx mice exhibit progressive muscle degeneration, which is exacerbated by persistent inflammation via the production of free radicals and cytotoxic cytokines (4). Myofiber loss is initially compensated by proliferation and fusion of resident myogenic precursor cells (satellite cells) with pre-existing myofibers that thereby enlarge in size. Ultimately, however, after repetitive cycles of muscle degeneration and persistent inflammation, dystrophic myofibers become gradually replaced by fibrotic and fat tissue (5; reviewed in 6-7)

Therapies based on restoration of dystrophin expression or the administration of dystrophin-positive stem cells are promising but still in the preclinical phase (8-14). Mounting evidence indicates a critical involvement of muscle extrinsic factors in DMD disease progression and the recovery of injured muscles. The composition of the basal lamina ECM around the necrotic myofibers can influence the overall repair process. Indeed, immediately after injury, a provisional fibrin-rich matrix and/or fibrin-rich hematoma forms between damaged fibers that provides a scaffold for tissue reorganization/reparative processes resulting in newly formed connective tissue altering contractile function, and a supportive matrix controlling the activity of infiltrating inflammatory cells (especially macrophages). While infiltrating inflammatory cells undoubtedly play a generally positive role in normal repair (e.g., by clearing myofiber debris), exuberant and persistent inflammatory cell action is likely to drive inopportune tissue reorganization in dystrophic muscle. These cells express several cytokines, growth factors, and other soluble mediators (e.g., TNFα, TGFβ, VEGF) that modulate the extent of myofiber degeneration as well as satellite cell-mediated regeneration (15-21). Thus, persistent and/or inappropriate ECM deposition around the myofiber is potentially pathogenic, and may promote inflammation in the damaged muscle tissue leading to inopportune tissue reorganization and loss of function. However, the specific matrix components and mechanisms that drive pathological inflammatory cell infiltration in the context of either muscular dystrophies or muscle damage remain largely unexplored.

The local conversion of soluble fibrinogen to a provisional fibrin matrix plays a seminal role in controlling blood loss following vascular injury and is understood to support reparative tissue reorganization (22-23). However, in addition to being a classic acute phase reactant, fibrin appears

to be a potent regulator of the innate immune system by serving as a matrix-associated regulator of inflammatory cell function. In macrophages, immobilized fibrin and fibrinogen (from here on we refer to both by the term “fibrin(ogen)”) induce activation of JNK and NF-kB via the $\alpha_M\beta_2$ (CD11b/CD18, Mac-1) integrin receptor, leading to the production of pro-inflammatory cytokines (24; reviewed in 25). Our previous studies showed that fibrin(ogen) and collagen matrices accumulated in diaphragms of aging mdx mice, while pharmacological fibrinogen depletion attenuated muscle fibrosis observed with age (24). However, the precise mechanism(s) by which fibrin(ogen) influences disease progression remain obscure.

In the present study, we show that fibrin(ogen), which is never detected outside of the vascular compartment in healthy muscle, is deposited in the muscle microenvironment immediately after injury, and upon disease onset in mdx mice. Using a combination of genetic and pharmacological approaches focused on fibrin(ogen), we directly tested the hypothesis that the severity of muscular dystrophy in mdx mice is dependent on fibrin(ogen) and that a mechanism supporting disease progression is coupled to the proinflammatory property of fibrin(ogen) linked to the $\alpha_M\beta_2$ binding motif. These studies establish for the first time that development of muscle pathology in mdx mice can be strongly attenuated by a simple fibrinogen mutation that has no influence on hemostasis and provide a proof-of-principle of the potential utility of interfering with the $\alpha_M\beta_2$-fibrin(ogen) interactions for treating DMD and other inflammatory myopathies.

RESULTS

GENETIC OR PHARMACOLOGICAL DEPLETION OF FIBRINOGEN ATTENUATES DEGENERATION, ENHANCES REGENERATION AND PRESERVES FUNCTION OF DYSTROPHIC MOUSE MUSCLE

To investigate whether fibrin(ogen) may directly control dystrophic muscle degeneration, we first analyzed its presence in limb muscles before and after the disease onset in mdx mice. Prior to disease onset (14 days of age), fibrinogen was undetectable by immunostaining in gastrocnemius muscle of mdx mice (Fig. 1 A). In contrast, at the first signs of disease (21 days of age), and especially at the disease peak (30 days of age), fibrin(ogen)-deposits were readily detectable in areas of muscle degeneration and inflammation (Fig. 1 A), remaining elevated thereafter. As fibrin(ogen) deposition was not detected in muscles from healthy age-matched wild type (WT) mice, these findings suggest that the accumulation of this provisional matrix protein specifically associates with dystrophinopathy in mdx mice.

To explore the importance of fibrin(ogen) on muscle disease, we bred mdx mice onto a fibrinogen-deficient background ($Fib^{-/-}$mdx mice) and analyzed the consequences of fibrinogen deficiency on dystrophic disease initiation and progression. Prior to 14 days of age, no evidence of muscle dystrophy was observed in cohorts of either $Fib^{-/-}$mdx or $Fib^{+/+}$mdx mice, a finding that is consistent with the absence of fibrin(ogen)-deposits in mdx muscle before disease onset (data not shown). As expected, at 1 month of age, fibrinogen-sufficient mdx mice, but not $Fib^{-/-}$mdx mice, exhibited obvious fibrin(ogen) deposition in damaged muscle areas (Fig. 1 B). However, more impressively, we observed significantly less muscle damage in $Fib^{-/-}$mdx mice of 1 and 2.5 month of age in comparison to aged-matched $Fib^{+/+}$mdx mice tracked in parallel, as indicated by the reduced degenerating muscle area and lower levels of serum creatine kinase (CK) (Fig. 1 C, and Fig. S1 A). $Fib^{-/-}$mdx mice also exhibited a higher frequency of larger central-nucleated regenerating myofibers (Fig. 1 D). In $Fib^{+/+}$mdx muscles, infiltrating macrophages were found in the areas where fibrin(ogen) deposition was prominent, whereas the number of macrophages was significantly reduced in muscle tissue from $Fib^{-/-}$mdx mice (Fig. 1 E). In a distinct but complementary model of chemically-induced muscle injury (cardiotoxin challenge), fibrinogen deficiency resulted in a similar dampening of macrophage infiltration (Fig. 1 F) to muscle tissue and an increase in the size of regenerating fibers (Fig. 1 G) to that observed in the mdx model. These results suggest that regardless of etiology, the loss of fibrin(ogen) resulted in more limited muscle inflammation and altered regeneration pattern.

As a complement to these genetics-based studies using mice with life-long fibrin(ogen) deficiency, we explored whether the severity of dystrophic disease was also diminished in mdx mice following the administration of an established pharmacological defibrinogenating agent, ancrod (24, 26-27). Here, when ancrod was administered to 12-day-old mdx mice and continued

until the age of 2.5 months the mice exhibited both reduced fibrin(ogen) deposition in muscle tissue relative to vehicle-treated control mdx mice (Fig. 2 A) and a significant overall protection against severe dystrophic pathology as shown by: (i) a reduction of 40% in the total area of muscle degeneration (Fig. 2 B, left), (ii) a diminution in circulating serum CK (Fig. 2 B, right), and (iii) enhanced fiber regeneration (indicated by the larger size of central-nucleated fibers; Fig. 2 C). Furthermore, fibrinogen depletion improved the physical performance of mdx mice, as shown by the preserved skeletal muscle strength (assessed by grip strength dynamometer tests) and the capacity of mdx mice to run at increasing high speed prior to exhaustion (Fig. 2 D). Thus, the genetic or pharmacological elimination of one regulator of tissue repair and inflammation, fibrin(ogen), is revealed a powerful modifier of degenerative muscle disease and protects mdx mice from functional muscle deterioration.

EXOGENOUS FIBRINOGEN IS SUFFICIENT TO INDUCE INFLAMMATION AND MUSCLE DEGENERATION IN FIBRINOGEN NULL MICE

Fibrin(ogen) can regulate inflammation in various conditions (28-31). Given the reduced presence of infiltrated macrophages in $Fib^{-/-}$mdx mice (see above), we sought to verify whether pharmacological depletion of fibrinogen exerts its beneficial effect, at least in part, by modulating inflammation. We therefore analyzed the macrophage distribution in the following three distinct types of areas corresponding to the initial stages of the degeneration/regeneration cycle: degenerating areas, characterized by areas of extensive myofiber degeneration/necrosis and ECM-deposition, and absence of regenerating myofibers (*phase I*); early regenerating areas, with small nascent myofibers and absence of necrotic fibers (*phase II*), and advanced regenerating areas containing well-defined, larger regenerating myofibers (*phase III*) (see Fig. S2 A). Fibrinogen depletion resulted in an overall reduction of infiltrating macrophages (Fig. S2 B left). A closer examination revealed that loss of fibrin(ogen) did not affect macrophage accumulation during the initial stage of myofiber degeneration/necrosis (*phase I*), but rather it caused a decrease in macrophage number in subsequent phases where fibers are attempting to regenerate (phases II/III; Fig. S2 B right). These findings are consistent with the prevailing concept that fibrin(ogen) is not required for leukocyte trafficking *per se*, but rather controls local leukocyte activation events that alter both cellular function and the expression of secondary proinflammatory cues. The aggravating effects of fibrin(ogen) on muscle degeneration/regeneration in the context of the chronic insult imposed by the mdx mutation could result, at least in part, from the expression of pro-inflammatory cytokines. Indeed, we found much reduced expression of TNFα, IL-6 and IL-1β in defibrinated mdx muscle compared to vehicle treatment (Fig. S2 C). A similar association between reduced macrophage infiltration and increased growth of regenerating myofibers was observed after

cardiotoxin injury in defibrinated WT mice (Fig. S2 D), supporting the conclusion that reduction of fibrin(ogen) levels attenuates inflammation in degenerating dystrophic muscle.

Although inflammatory macrophage infiltrates are a prominent feature of provisional extracellular matrices early after muscle injury, reviewed in (7, 32), neither the specific matrix components that control macrophage function within damaged muscle tissue nor the consequences for muscle disease/repair of limiting function at the level of the provisional matrix-leukocyte interface have been defined. Given that we observed fibrin(ogen) deposition rapidly following muscle damage (Fig. 3 A) and that depletion of fibrin(ogen) could ameliorate local muscle damage in both a genetic model of muscle dystrophy and a chemically-induced model of inflammatory muscle damage, we hypothesized that fibrin(ogen) could be the early signal that triggers activation of macrophages within provisional matrices. To directly determine whether fibrin(ogen) deposition was a specific driver of macrophage activity in muscle, we injected fibrinogen or vehicle into the right and left tibialis muscles, respectively, of $Fib^{-/-}$ mice. Challenged muscle was then examined for evidence of both fibrin(ogen)-mediated macrophage activation events as well as a tissue-damage/repair-like response. As shown in Figure 3 B, local fibrin deposition was sufficient to induce an acute inflammatory reaction in the $Fib^{-/-}$ mouse tibialis muscle as shown by significantly higher macrophage cell numbers within fibrinogen-challenged muscle tissue relative to the saline-injected contralateral tibialis muscle. The fibrin(ogen)-induced inflammation (and ECM accumulation, Fig. 3 B) was subsequently followed by degeneration (Fig. 3 C left) and the appearance of small eMHC positive regenerating myofibers in $Fib^{-/-}$ mice (Fig. 3 C right). Thus, fibrin(ogen) deposition is capable of triggering a cascade of events typical of a muscle injury-regeneration response, including inflammatory cell infiltration, ECM accumulation, muscle degeneration and new myofiber formation.

SPECIFIC INTERACTION OF FIBRIN(OGEN) WITH $\alpha_M\beta_2$ INTEGRIN RECEPTOR ON MACROPHAGES PROMOTES MDX MUSCLE DEGENERATION

Since leukocyte integrin receptor CD11b/CD18/$\alpha_M\beta_2$ engagement of immobilized fibrin(ogen) has the potential to regulate cytokine expression in other settings (33-36), we sought to examine the contribution of the fibrin(ogen)–$\alpha_M\beta_2$ interactions to the inflammatory response and muscle degeneration in mdx mice. To this end, we employed $Fib\gamma^{390-396A}$ mice expressing a mutant form of fibrinogen that retains full clotting function but lacks the integrin $\alpha_M\beta_2$ binding motif (33). Here, we intercrossed $Fib\gamma^{390-396A}$ knock-in mice with mdx mice and compared the extent of muscle inflammation and degeneration in cohorts of mdx mice carrying either fibrinogen-$\gamma^{390-396A}$ or wild-type fibrinogen. $Fib\gamma^{390-396A}$mdx mice were indistinguishable from control mdx mice before disease onset (14 days after birth) (not shown). However, at 2.5 months of age, $Fib\gamma^{390-396A}$mdx mice

showed appreciably reduced macrophage infiltration relative to age-matched mdx mice (Fig. 4 A and B). Notably, Fib$\gamma^{390-396A}$mdx mice exhibited more limited myofiber degeneration area, reduced serum CK levels (Fig. 4 B), larger size regenerating fibers (Fig. 4 C), and preserved locomotor activity (Fig. 4 D). Thus, muscle disease can be attenuated and muscle function preserved despite a fundamental initiating genetic insult for muscular dystrophy by imposing an alteration of fibrin(ogen) that limits $\alpha_M\beta_2$-mediated leukocyte activation events but does not compromise hemostasis. The general findings were again extended to the model of chemically-induced muscle injury where, like fibrinogen-deficient mice, Fib$\gamma^{390-396}$ knock-in mice exhibited an appreciable phenotypic benefit relative to control mice in the form of reduced presence of macrophages (Fig. 4 E) and larger regenerating myofibers (Fig. 4 F).

TREATMENT WITH THE FIB$\gamma^{377-395}$ PEPTIDE LIMITS MACROPHAGE ACTIVATION AND AMELIORATES MDX MUSCULAR DYSTROPHY PROGRESSION

Previous studies have shown that a peptide corresponding to Fib$\gamma^{377-395}$ is capable of impeding fibrin(ogen)-mediated leukocyte binding via $\alpha_M\beta_2$ and secondary activation events (34, 37-38). We confirmed that a synthetic peptide corresponding to fibrinogen gamma chain residues 377-395, but not a scramble peptide, specifically inhibited the in vitro activation of primary macrophages in response to fibrinogen stimulation, as measured by the expression of TNFα, IL-6 and IL-1β cytokines. Similar inhibitory effects were obtained using a specific blocking antibody against $\alpha_M\beta_2$ integrin (Fig. 5 A). Interestingly, treatment of macrophages with Fib$\gamma^{377-395}$ peptide also blocked fibrinogen-induced NF-κB activation in vitro (not shown), reinforcing the reported induction of cytokines by fibrin(ogen) through a $\alpha_M\beta_2$-dependent NF-κB axis (24, 39-40). As a complement to our studies of Fib$\gamma^{390-396A}$ mice, we examined whether the Fib$\gamma^{377-395}$ peptide could also limit pro-inflammatory processes and the development of dystrophy in mdx mice. We treated 2-month-old mdx mice with a Fib$\gamma^{377-395}$ peptide, or a scramble peptide, for a three-week period. Neither mice treated with the scrambled peptide nor the Fib$\gamma^{377-395}$ peptide showed any signs of hemorrhage either grossly or within muscle tissue in microscopic analyses. However, while the scrambled peptide predictably did not alter disease progression, mdx mice treated with the Fib$\gamma^{377-395}$ peptide showed reduced inflammation and muscle degeneration, as indicated by diminished macrophage infiltrates (Fig. 5 B), lower degenerating areas (Fig. 5 C, left), and reduced serum CK levels (Fig. 5 C, right). These phenotypic benefits were also associated with larger regenerating myofibers (Fig. 5 D), decreased expression of pro-inflammatory cytokines (Fig. 5 E) and improved motor performance (Fig. 5 F). Collectively, these results show that in vivo treatment with the Fig$\gamma^{377-395}$ peptide attenuated the severity of muscular dystrophy without imposing hemorrhagic risk.

FIBRINOGEN REGULATES SATELLITE CELL-DEPENDENT MUSCLE REGENERATION VIA DIRECT AND INDIRECT MECHANISMS

Muscles of Fig$\gamma^{390\text{-}396A}$mdx mice contained larger central-nucleated myofibers compared to aged-matched mdx control mice (Fig. 4 C), suggesting that the selective blockade of the fibrin(ogen)/$\alpha_M\beta_2$-mediated inflammatory/degenerative processes also promoted myofiber regeneration. Since it is well-established that muscle regeneration relies on activation and differentiation of satellite cells (41-42), we explored whether cytokines produced in response to $\alpha_M\beta_2$-mediated macrophage engagement of fibrinogen altered muscle satellite cell functions. As shown in Figure 6 A, conditioned medium (CM) from fibrinogen-stimulated macrophages, but not from non-stimulated cells, induced hyperproliferation of satellite cells based on BrdU incorporation assays. Addition of this macrophage CM also reduced the satellite cell differentiation potential, as shown by analyses of myogenin and eMHC expression (Fig. 6 B and 6 C, respectively). Importantly, these effects were significantly reversed by addition of TNFα and IL-1β neutralizing antibodies to the CM of fibrinogen-treated macrophages, demonstrating that, indeed, fibrinogen-induced pro-inflammatory cytokines underlied the altered myogenesis in a paracrine fashion (Fig. 6). Together, these results suggest that the proinflammatory milieu generated through persistent fibrin(ogen) within the dystrophic muscle microenvironment indirectly limits myofiber regeneration by inhibiting satellite cell activity. However fibrin(ogen) may also directly alter satellite cell–dependent muscle tissue repair, and this concept is compatible with immunohistochemical findings showing that fibrin(ogen) deposition in mdx mouse muscle was initimately associated, and often surrounded, activated (MyoD$^+$) satellite cells (Fig. 7 A). To directly test whether fibrin(ogen) might alter directly satellite cell functions, we cultured satellite cells in the absence or presence of fibrinogen and assessed their proliferation and fusion properties (Fig. 7 B and C). Treatment of satellite cells with increasing amounts of fibrinogen induced a hyperproliferative effect compared to untreated cells, as shown by satellite cell count following 3 days in culture and by BrdU incorporation (Fig. 7 B). Consistent with the reported expression in myoblasts of $\alpha_V\beta_3$ integrin (43-45) a known fibrinogen binding receptor (23), we found that incubation of satellite cells with either an RGD cyclic peptide that specifically interferes with $\alpha_V\beta_3$ or an anti-α_V antibody reversed the fibrinogen-induced satellite cell hyperproliferation (Fig. 7 B, right). In addition, immunostaining for eMHC in satellite cells cultured in differentiation medium showed reduced myogenic fusion in the presence of fibrinogen (Fig. 7 C). These results further support the idea that excessive and/or persistent deposition of fibrin(ogen) might impair regeneration in mdx muscle by both direct and indirect mechanisms acting on satellite cells.

ASSOCIATION OF FIBRIN(OGEN) DEPOSITION AND MACROPHAGE INFILTRATES IN DYSTROPHIC MUSCLE OF DMD PATIENTS

Prompted by our findings that fibrin(ogen) regulates inflammation and muscle degeneration/regeneration in mdx dystrophic disease, we analyzed tissue biopsies of degenerating muscle from DMD patients for the presence of fibrin(ogen) deposits and inflammatory cell infiltrates. Compared to muscle biopsies of healthy subjects, in which fibrin(ogen) positivity was only observed in capillaries surrounding myofibers, DMD muscles showed significant fibrin(ogen) accumulation correlating with muscle damage. Immunohistochemical analyses using a $\alpha_M\beta_2$ antibody also showed a prominent presence of macrophages in the same degenerating areas occupied by fibrin(ogen) (Fig. 8 A and Fig. S3) in human dystrophic muscles, but were absent in biopsies from healthy individuals. Thus, a linkage between exuberant and recurrent fibrin(ogen) deposition and secondary inflammatory changes driving muscle disease progression may be a common feature of both mdx mice and human DMD.

DISCUSSION

Despite intense research efforts, Duchenne muscular dystrophy (DMD) is still an incurable and fatal degenerative muscle disorder that demands novel experimental and therapeutic advances. The present study explores a new mechanistic and therapeutic dimension by examining the molecular link between fibrin(ogen) deposition within persistently challenged muscle and inflammation-driven muscle damage, tissue reorganization and function loss. We provide direct evidence that fibrin(ogen), which is never present in normal muscle but rapidly accumulates in dystrophic muscle secondary to persistent tissue disruption and vascular leak, is a critical factor for inflammation-mediated DMD progression. Imposing either a genetic or pharmacological depletion of fibrinogen reduced macrophage numbers and activation in injured and dystrophic muscle and enhanced repair, while preserving locomotor capacity. However, more detailed studies revealed that muscle dystrophy pathology could also be ameliorated and muscle function preserved by interventions at the level of fibrinogen that do not impose any hemostatic alteration or hemorrhagic risk. Specifically, the simple elimination of the $\alpha_M\beta_2$ binding motif on the fibrin(ogen) gamma chain that drives pro-inflammatory functions, but is irrelevant to fibrin polymer formation, sufficed to alleviate disease severity in mdx dystrophic muscle. Conversely, delivery of exogenous fibrinogen into intact muscle of fibrinogen-null mice caused a classical inflammatory-tissue repair response. The relevance of these findings to human disease is underscored by the finding that fibrin(ogen) accumulation was positively associated with inflammation in degenerating muscles of DMD patients. Hence, selectively targeting fibrin(ogen) inflammatory functions may represent a promising therapeutic strategy for DMD.

The fact that fibrin(ogen) depletion affected several distinct aspects of muscle disease in mdx mice, implies that recurrent fibrin deposition within the ECM may influence the progression of muscle disease through multiple mechanisms (see Fig. 8 B). Vascular damage early after disease onset in dystrophic muscle and secondary fibrin(ogen) accumulation in the ECM may be an early driver of the inflammatory changes known to exacerbate muscular dystrophy (17, 20-21, 46-49). Under this working hypothesis, intramuscular fibrin(ogen) deposits serve as temporospatial cue controlling local activation events in macrophages and other inflammatory cells that express $\alpha_M\beta_2$, reviewed in (50), and recurrent and/or exuberant fibrin(ogen) within diseased muscle tissue promotes counterproductive inflammatory tissue degeneration. Our results demonstrate that upon fibrin(ogen) engagement, macrophages increase the expression of pro-inflammatory cytokines, including IL-1β, TNFα and IL-6 in vitro and in vivo, in a $\alpha_M\beta_2$-dependent manner. The presence of fibrin(ogen) appears to regulate the expression of cytokines known to promote muscle degeneration and impair regeneration, such as TNFα (17, 49). Limiting these responses via experimentally-imposed suppression of fibrin(ogen)-$\alpha_M\beta_2$ engagement by macrophages and other inflammatory cells may largely explain the reduced pathological changes observed in mdx muscle.

Our data do not exclude other fibrinogen-mediated effects on inflammatory cells such as $\alpha_M\beta_2$-mediated inhibition of inflammatory cell apoptosis (39-40) and the increased release of free radicals (47, 51-52).

Previous reports have shown that macrophage depletion or interference with pro-inflammatory cytokines transiently attenuated muscle dystrophy in mdx mice (20, 53-54; reviewed in 7, 32, 55). Our present findings further underscore the relevance of the $\alpha_M\beta_2$ integrin receptor in macrophage activation in DMD and directly establish for the first time that the engagement of $\alpha_M\beta_2$ with one of its ligands, fibrin(ogen), an early component of the muscle provisional matrix after injury, is a critical regulatory event in dystrophic muscle pathology. We show that mice bearing an endogenous fibrinogen γ chain gene with a specific mutation in the $\alpha_M\beta_2$ binding region ($Fib\gamma^{390-396A}$ mice), which does not affect the clotting function of fibrinogen and does not limit the engagement of $\alpha_M\beta_2$ with other ligands (33-34), are significantly protected from acute muscle injury and dystrophic disease progression. Furthermore, the effective amelioration of muscle dystrophy in mdx mice treated with the $Fib\gamma^{377-395}$ peptide demonstrates that inflammatory functions of fibrin(ogen) can, at least in principle, be pharmacologically suppressed, thus presenting an alternative treatment paradigm for impeding DMD disease progression.

Impeding macrophage $\alpha_M\beta_2$/fibrin(ogen) binding could also enhance muscle regeneration, which is primarily mediated by activation of satellite cells, localized along the basal lamina. This effect might again be related to the inhibition of macrophage activation. Interestingly, we also found that fibrin(ogen) was deposited in the fibronectin$^+$ and laminin$^+$ ECM basal lamina of regenerating mdx muscle, where it physically entrapped satellite cells. Further, we demonstrated that fibrinogen regulates the proliferation and differentiation potential of satellite cells in culture through an $\alpha_v\beta_3$-dependent mechanism. Thus, fibrin(ogen) depletion may promote regeneration at least in part by indirectly attenuating inflammation, and possibly by diminishing direct deleterious effects of persisting fibrinogen on satellite cell functions.

Collectively, we propose that the development of exuberant and recurrent fibrin-rich matrices within challenged muscle tissue establishes a counterproductive inflammatory environment through $\alpha_M\beta_2$-mediated leukocyte activation events as well as a counterproductive environment for muscle tissue regeneration. Consistent with this, our analysis on DMD patient samples suggests an association between fibrin(ogen) deposition and the presence of macrophages in degenerating dystrophic muscle. Interestingly, interference with the fibrin(ogen)/macrophage axis was recently shown to ameliorate neurodegeneration and halt demyelination in a mouse model of multiple sclerosis (34), to protect from collagen-induced arthritis (35) and colitis-associated colon cancer in mice (36). Alzheimer disease has also been associated to fibrinogen deposition and inflammation (56-57). It is therefore possible that targeting fibrinogen-

$\alpha_M\beta_2$ interactions could represent a quite broad strategy for inhibiting macrophage activation in neurodegenerative diseases coursing with inflammation. In this regard, our study provides a compelling proof-of-principle that the sole blockage of fibrinogen binding to $\alpha_M\beta_2$ on macrophages via therapeutic administration of the Fib$\gamma^{377-395}$ peptide improved muscle function in mdx mice. Although the activation of macrophages plays a central role in the pathogenesis of muscular dystrophies, reviewed in (6-7), to the best of our knowledge agents that selectively inhibit macrophage inflammatory activation have not been developed and tried in this pathology. A potential advantage of a fibrin(ogen)/macrophage interaction-based approach over current anti-inflammatory strategies is that interfering with $\alpha_M\beta_2$-fibrin(ogen) is likely to impose only a local block on the activation (and recruitment) of macrophages, i.e. within the dystrophic muscle where fibrin(ogen) is deposited. Since no therapies correcting the primary defect in DMD (i.e. dystrophin replacement or rescue) are currently available, strategies selectively targeting fibrin(ogen)/inflammatory cell signaling, without affecting its pro-coagulant properties, may constitute an attractive alternative for DMD disease treatment.

MATERIALS AND METHODS

Generation of double-mutant mice

Fibrinogen (Fib) knock-out male mice (58) were crossed with mdx female mice, Jackson Laboratories (USA). Male F1 mice were bred with mdx female mice, and their F2 heterozygous ($Fib^{+/-}$) male and female offspring was intercrossed. The resulting F3 generation showed the expected Mendelian distribution of $Fib^{+/+}$, $Fib^{+/-}$ and $Fib^{-/-}$ genotypes, all of them in an mdx background. The Fib genotypes were confirmed by polymerase chain reaction (PCR) of ear biopsy genomic DNA, as previously described (58). The mdx genotype was confirmed by Western blotting of muscle biopsies, using an anti-dystrophin antibody (Novocastra, UK, 1:200). Fib-gamma(390-396A) ($Fib\gamma^{390-396A}$) knock-in mice (33) were generated from double heterozygous matings to produce homozygous $Fib\gamma^{390-396A}$ mice. Male $Fib\gamma^{390-396A}$ mice were sequentially intercrossed with mdx female mice, as described above, to generate double-mutant mice. All animal experiments were approved by the Catalan Government of Animal Care Committee.

Morphometric analysis

At selected times, muscles of vehicle and ancrod-treated mdx mice, $Fib^{+/+}$, $Fib^{-/-}$, $Fib\gamma^{390-396A}$, $Fib^{+/+}$mdx, $Fib^{-/-}$mdx, and $Fib\gamma^{390-396A}$mdx mice were removed after cervical dislocation, frozen and stored at –80º C prior to analysis. 10 µm sections were collected from the mid-belly of muscles and stained with hematoxylin/eosin (H&E). The percentage of muscle degeneration was determined by morphometrical analysis of digital photomicrographs of H&E stained cryosections. Areas of necrosis and degeneration were identified by the presence of pale-stained myofibers, with irregular shape and often fragmented sarcoplasm. These areas contained few myonuclei and inflammatory cells were not conspicuous. Evans Blue Dye staining, a vital stain of myofibre permeability (59) showed that degenerating areas identified with H&E were composed of damaged fibers that had become permeable owing to muscular dystrophy (Fig. S1). The areas of degeneration on each individual sample were measured using the public domain ImageJ software on calibrated micrographs and were expressed as a percentage of the total muscle cross-sectional area (CSA). Myofibers CSA was determined as an indicator of muscle growth and regeneration. All analyses and photography were performed on a Leica DC 500 microscope equipped with a video camera. All parameters relative to myofiber CSA were measured using the ImageJ program.

Biochemical and functional assessment of muscle

Serum creatine kinase (CK) was measured with the indirect CK colorimetric assay kit and standards (Thermo Electron, USA). Grip strength assay: Limbs grip strength was measured as tension force using a computerized force transducer (Grip Strength Meter, Bioseb). Three trials of 3 measurements per trial were performed for each animal with a few minutes resting period between trials. The average tension force (grams) was calculated for each group of mice. Treadmill assay: the treadmill apparatus (Treadmill, Panlab) consisted of a motor-driven belt varying in terms of speed and slope. At the end of the treadmill,

an electrified grid was placed, on which footshocks (0.6 mA) were administered whenever the mice fell off the belt. The last week before sacrifice, after one daily acclimation session of 20 min at 6m/min for 2 days, all mice were subjected to exhaustion treadmill tests at 5° inclination. Each test was repeated twice at a temporal distance of 4 days and results averaged. The following scheme was adopted: 5 min at 5 m/min followed by incremental increase of speed of 1 m/min every minute until exhaustion. Exhaustion was defined as spending time on the shocker plate without attempting to re-engage the treadmill within 20 s. The individual and the average times (min) and distances (meters) to exhaustion of running were measured.

Induction of muscle regeneration

Regeneration of skeletal muscle was induced by intramuscular injection of 300 µl of 10^{-5} M cardiotoxin (CTX) (Latoxan, France) in the gastrocnemius muscle group of the mice, usually of 8-12 weeks of age. This concentration and volume were chosen to ensure maximum degeneration of the myofibers. The experiments were performed in right hind limb muscles, and contralateral intact muscles were used as control. Morphological and biochemical examinations were performed at the indicated days after injury.

Systemic defibrination

12 days-old mdx mice were daily injected intraperitoneally with ancrod (Sigma, 1-3 U ancrod/day) or with a saline solution for 60 days, and killed at 2.5 months of age. Muscles were dissected and frozen prior to analysis.

Systemic delivery of Fib$\gamma^{377-395}$ peptide

Fibrinogen $\gamma^{377-395}$ peptide (Y S M K E T T M K I I P F N R L S I G ; Azco Pharmchem) or scramble peptide (K M M I S Y T F P I E R T G L I S N K ; Azco Pharmchem) was resuspended in 0.9% NaCl at a concentration of 3 mg/ml, as described (34). Peptides were delivered intraperitoneally every other day into 2 month-old mdx mice over the course of three weeks.

Intramuscular fibrinogen delivery

$Fib^{-/-}$ mice of 8-12 weeks of age were used for intramuscular injection of fibrinogen or saline. Fibrinogen (Calbiochem) was dissolved in endotoxin-free distilled water, diluted to 9 mg/ml with saline, aliquoted and kept at 37°C. Fibrinogen (50µl of 9 mg/ml) or saline was injected with a 10µl Hamilton syringe attached to a 33-gauge needle into mouse tibialis anterior muscles. Samples were obtained at the indicated time points.

Analysis of muscle macrophages by FACS

Hind-limb muscles were collected and weighed. Muscles were dissociated by incubation in DMEM containing pronase 0.05% (Calbiochem) at 37°C for 45 min twice, filtered, and counted. Cells were separated using a Percoll gradient and stained with FITC-conjugated anti-CD45, allophycocyanin-Cy7–conjugated F4/80 antibody (BD Pharmingen). Cells were sorted using a cell sorter (FACS Aria II; BD). Total number of cells was normalized by milligram of wet tissue.

Immunohistochemistry

The following primary antibodies were used for immunohistochemistry: rat anti-F4/80 (Serotec, 1:200), goat anti-Fibrin/ogen (Nordic, 1:100), rabbit anti-MyoD (Santa Cruz Biotechnology, 1:20), rabbit anti-Fibronectin (Sigma, 1:40), rabbit anti-Laminin (Sigma, 1:50); monoconal anti-human fibrin/ogen antibody (Accurate Chemical & Scientific Corporation, WESTBURY, NY), clone NYBT2G1, 1:200, and rat anti-mouse α_M / CD11b (ebioscience 1:100), eMHC (F1.652, neat hybridoma supernatant; Developmental Studies Hybridoma Bank). Depending on the antibody, immunohistochemistry was performed with the TSA Cyanine 3 system (PerkinElmer Life Sciences) or as previously described (60). Control experiments without primary antibody demonstrated that signals observed were specific (not shown).

Cell culture and isolation of primary cells

Isolation and culture of primary macrophages: Bone-marrow derived macrophages (BMDMs) were obtained from mdx mice and cultured as previously described (24, 61). In brief, bone marrow cells were flushed from the femurs of mice. Cells were differentiated in DMEM supplemented with 20% heat-inactivated FCS and 30% L929 supernatants containing macrophage-stimulating factor (MCSF) for 5–7 days. Cells were harvested and plated at a density of 2–4x10^5 per ml in RPMI supplemented with 5% FBS. At 24–48 h after being replated, cells were stimulated for various times with LPS (10 ng/ml; Sigma). Conditioned medium (CM) from WT BMDMs was obtained stimulating cell cultures for with Fibrinogen (0.5 mg/ml; Sigma). When indicated, fibrinogen-stimulated macrophages were also treated with 200 μM of $\gamma^{377\text{-}395}$ peptide (a concentration shown to inhibit adhesion of $\alpha_M\beta_2$ / Mac-1–overexpressing cells to immobilized fibrinogen – (62), 200 μM of scramble peptide. When indicated, CM was supplemented with blocking antibodies anti-IL-1β (30 ng/ml; R&D Systems) or anti-TNFα (50 ng/ml; BD Pharmingen) or unspecific IgG.

Isolation and culture of muscle satellite cells: Hindlimb muscles from mice were excised, separated from adipose and connective tissue, minced into coarse slurry, and then digested for 1 h with 0.1% pronase (Sigma) in DMEM at 37°C with mild agitation. The digest was then mechanically dissociated by repeated trituration followed by filtration through a 100-mm vacuum filter (Millipore). The filtered digest was centrifuged through an isotonic Percoll gradient (60% overlaid with 20%). Mononucleated cells in the Percoll interface were collected and resuspended in Ham's F10 medium supplemented with 20% FCS, 100U/ml penicillin, 100mg/ml streptomycin, 0.001% Fungizone and 5 ng/ml bFGF

(GM). Primary satellite cell cultures were maintained on a routinary basis on collagen-coated dishes in GM. The medium was changed daily and cultures were passaged 1:3 as they reached 60-70% confluence. Experiments were performed by plating cells on Matrigel (BD Biosciences) Basement Membrane Matrix coated dishes. To maintain the primary characteristics of the cells, all experiments were performed using cultures that had undergone between four and seven passages. All experiments were performed with independent cell isolates from at least three different animals for each genotype. To induce muscle differentiation and fusion, GM was replaced by differentiation medium DM (DMEM supplemented with 2% horse serum, 2 mM L-glutamine, 100 U/ml penicillin, 100 mg/ml streptomycin and 0.001% Fungizone) at satellite cell subconfluence.

For detection of S-phase cells, satellite cells were cultured in GM, and cultures were pulsed with bromodeoxyuridine (BrdU, Sigma) for hours prior to fixation in 3.7% formaldehyde for 10 minutes and were immunostained using anti-BrdU antibody (Oxford Biotech) and a specific secondary biotinylated goat anti-rat antibody (Jackson Inmunoresarch Laboratories), followed by quantification (see 63). For fusion analysis, cells were immunostained with anti-eMHC antibody and nuclei within the eMHC positive myofibers were quantified (see 63). When indicated, CM of cultured macrophages, control non specific RGD peptide (GRGDNP; Biomol) or the cyclic RGD peptide (GpenGRGD; Bachem; 100 nM) or an alphaV neutralizing antibody (20 μg/ml; Chemicon), was added.

RNA isolation and quantitative RT-PCR

RNA was analyzed by quantitative reverse transcription-polymerase chain reaction (RT-PCR). Total RNA was isolated from cells or muscle tissue using Tripure reagent (Roche Diagnostic Corporation). DNase digestion of 10 µg of RNA was performed using 2 U DNase (Turbo DNA-free™, Ambion). Complementary DNA was synthesized from 2 µg of total RNA using the First-Strand cDNA Synthesis kit (Amersham Biosciences). PCRs were performed on a LightCycler® 2.0 or in a LightCycler® 480 System using a Light Cycler® FastStart DNA Master PLUS SYBR Green I or Light Cycler® 480 SYBR Green I Master (Roche Diagnostic Corporation) respectively and specific primers shown in Supplement table 1. Thermocycling conditions were as follow: initial step of 10 min at 95ºC, then 45 cycles of 15s denaturation at 94ºC, 10s annealing at 60ºC and 15s extension at 72ºC. Reactions were run in triplicate, and automatically detected threshold cycle (Ct) values were compared between samples. Transcripts of the ribosomal protein L7 gene were used as endogenous normalization control. qPCRs primers:

eMHC, 5'-AAAAGGCCATCACTGACGC-3' and 5'-CAGCTCTCTGATCCGTGTCTC-3'

Myogenin, 5'-GGTGTGTAAGAGGAAGTCTGTG-3' and 5'-TAGGCGCTCAATGTACTGGAT-3'

TNFα, 5'-CGCTCTTCTGTCTACTGAACTT-3' and 5'-GATGAGAGGGAGGCCATT-3'

IL-1β, 5'-CCAAAATACCTGTGGCCTTGG-3'and 5'-GCTTGTGCTCTGCTTGTGAG-3'

IL-6, 5'-GAGGATACCACTCCCAACAGACC-3' and 5'- AAGTGCATCATCGTTGTTCATACA-3'

L7, 5'-GAAGCTCATCTATGAGAAGGC-3' and 5'-AAGACGAAGGAGCTGCAGAAC-3'.

Statistical analysis

Data are presented as mean ± SEM. All quantitative data were analyzed with Prism software (GraphPad Software) for statistical analyses. One-way analysis of variance and Dunnett's test was used for multiple comparisons. Nonparametric Mann Whitney test was used for single comparisons of unmatched groups. $P<0.05$ was considered statistically significant.

ACKNOWLEDGMENTS

We thank Drs. M. Dewerchin, M. Twja and E. Perdiguero for excellent discussions and advice, M. Jardí, S. Gutarra, J. Guerra and V. Lukesova for technical support, J. Martín-Caballero for assistance in animal experimentation. We are indebted to Dr. J. Colomer (Hospital Sant Joan de Deu, Barcelona, Spain) for DMD muscle biopsies. The authors acknowledge funding from MICINN (SAF2009-09782, FIS-PS09/01267, PLE2009-0124, CIBERNED), AFM, Fundación Marató-TV3/R-Pascual, MDA, EU-FP7 (Myoage, Optistem and Endostem). J.L.D. is supported by NIH grants AR049822 and HL085357. M.J.F is supported by NIH grant R01 AR056990.

No conflict of interest exists

REFERENCES

1 Campbell, K.P. (1995) Three muscular dystrophies: loss of cytoskeleton-extracellular matrix linkage. *Cell*, **80**, 675-679.

2 Sicinski, P., Geng, Y., Ryder-Cook, A.S., Barnard, E.A., Darlison, M.G. and Barnard, P.J. (1989) The molecular basis of muscular dystrophy in the mdx mouse: A point mutation. *Science*, **244**, 1578-1580.

3 Durbeej, M. and Campbell, K.P. (2002) Muscular dystrophies involving the dystrophin-glycoprotein complex: an overview of current mouse models. *Curr Opin Genet Dev*, **12**, 349-361.

4 Tidball, J.G. (2005) Mechanical signal transduction in skeletal muscle growth and adaptation. *J Appl Physiol*, **98**, 1900-1908.

5 Stedman, H.H., Sweeney, H.L., Shrager, J.B., Maguire, H.C., Panettieri, R.A., Petrof, B., Narusawa, M., Leferovich, J.M., Sladky, J.T. and Kelly, A.M. (1991) The mdx mouse diaphragm reproduces the degenerative changes of Duchenne muscular dystrophy. *Nature (London)*, **352**, 536-539.

6 Serrano, A.L., Mann, C.J., Vidal, B., Ardite, E., Perdiguero, E. and Munoz-Canoves, P. (2011) Cellular and molecular mechanisms regulating fibrosis in skeletal muscle repair and disease. *Curr Top Dev Biol*, **96**, 167-201.

7 Mann, C.J., Perdiguero, E., Kharraz, Y., Aguilar, S., Pessina, P., Serrano, A.L. and Munoz-Canoves, P. (2011) Aberrant repair and fibrosis development in skeletal muscle. *Skelet Muscle*, **1**, 21.

8 Goyenvalle, A., Vulin, A., Fougerousse, F., Leturcq, F., Kaplan, J.C., Garcia, L. and Danos, O. (2004) Rescue of dystrophic muscle through U7 snRNA-mediated exon skipping. *Science*, **306**, 1796-1799.

9 Shi, X. and Garry, D.J. (2006) Muscle stem cells in development, regeneration, and disease. *Genes & development*, **20**, 1692-1708.

10 Montarras, D., Morgan, J., Collins, C., Relaix, F., Zaffran, S., Cumano, A., Partridge, T. and Buckingham, M. (2005) Direct isolation of satellite cells for skeletal muscle regeneration. *Science*, **309**, 2064-2067.

11 Sampaolesi, M., Blot, S., D'Antona, G., Granger, N., Tonlorenzi, R., Innocenzi, A., Mognol, P., Thibaud, J.L., Galvez, B.G., Barthelemy, I. *et al.* (2006) Mesoangioblast stem cells ameliorate muscle function in dystrophic dogs. *Nature*, **444**, 574-579.

12 Gregorevic, P., Allen, J.M., Minami, E., Blankinship, M.J., Haraguchi, M., Meuse, L., Finn, E., Adams, M.E., Froehner, S.C., Murry, C.E. *et al.* (2006) rAAV6-microdystrophin preserves muscle function and extends lifespan in severely dystrophic mice. *Nature medicine*, **12**, 787-789.

13 Welch, E.M., Barton, E.R., Zhuo, J., Tomizawa, Y., Friesen, W.J., Trifillis, P., Paushkin, S., Patel, M., Trotta, C.R., Hwang, S. *et al.* (2007) PTC124 targets genetic disorders caused by nonsense mutations. *Nature*, **447**, 87-91.

14 Gargioli, C., Coletta, M., De Grandis, F., Cannata, S.M. and Cossu, G. (2008) PlGF-MMP-9-expressing cells restore microcirculation and efficacy of cell therapy in aged dystrophic muscle. *Nature medicine*, **14**, 973-978.

15 Chen, S.E., Gerken, E., Zhang, Y., Zhan, M., Mohan, R.K., Li, A.S., Reid, M.B. and Li, Y.P. (2005) Role of TNF-{alpha} signaling in regeneration of cardiotoxin-injured muscle. *Am J Physiol Cell Physiol*, **289**, C1179-1187.

16 Collins, R.A. and Grounds, M.D. (2001) The role of tumor necrosis factor-alpha (TNF-alpha) in skeletal muscle regeneration. Studies in TNF-alpha(-/-) and TNF-alpha(-/-)/LT-alpha(-/-) mice. *J Histochem Cytochem*, **49**, 989-1001.

17 Grounds, M.D. and Torrisi, J. (2004) Anti-TNFalpha (Remicade) therapy protects dystrophic skeletal muscle from necrosis. *Faseb J*, **18**, 676-682.

18 Germani, A., Di Carlo, A., Mangoni, A., Straino, S., Giacinti, C., Turrini, P., Biglioli, P. and Capogrossi, M.C. (2003) Vascular endothelial growth factor modulates skeletal myoblast function. *Am J Pathol*, **163**, 1417-1428.

19 Brunelli, S., Sciorati, C., D'Antona, G., Innocenzi, A., Covarello, D., Galvez, B.G., Perrotta, C., Monopoli, A., Sanvito, F., Bottinelli, R. *et al.* (2007) Nitric oxide release combined with nonsteroidal antiinflammatory activity prevents muscular dystrophy pathology and enhances stem cell therapy. *Proc Natl Acad Sci U S A*, **104**, 264-269.

20 Wehling, M., Spencer, M.J. and Tidball, J.G. (2001) A nitric oxide synthase transgene ameliorates muscular dystrophy in mdx mice. *J Cell Biol*, **155**, 123-131.

21 Tidball, J.G. (2005) Inflammatory processes in muscle injury and repair. *Am J Physiol Regul Integr Comp Physiol*, **288**, R345-353.

22 Pereira, M., Rybarczyk, B.J., Odrljin, T.M., Hocking, D.C., Sottile, J. and Simpson-Haidaris, P.J. (2002) The incorporation of fibrinogen into extracellular matrix is dependent on active assembly of a fibronectin matrix. *Journal of cell science*, **115**, 609-617.

23 Rybarczyk, B.J., Lawrence, S.O. and Simpson-Haidaris, P.J. (2003) Matrix-fibrinogen enhances wound closure by increasing both cell proliferation and migration. *Blood*, **102**, 4035-4043.

24 Vidal, B., Serrano, A.L., Tjwa, M., Suelves, M., Ardite, E., De Mori, R., Baeza-Raja, B., Martinez de Lagran, M., Lafuste, P., Ruiz-Bonilla, V. *et al.* (2008) Fibrinogen drives dystrophic muscle fibrosis via a TGFbeta/alternative macrophage activation pathway. *Genes & development*, **22**, 1747-1752.

25 Ryu, J.K., Davalos, D. and Akassoglou, K. (2009) Fibrinogen signal transduction in the nervous system. *J Thromb Haemost*, **7 Suppl 1**, 151-154.

26 Bell, W., Shapiro, S., Martinez, J. and Nossel, H.L. (1978) The effects of ancrod, the coagulating enzyme from the venom of Malayan pit viper (A. Rhodostoma) or prpthrombin and fibrinogen metabolism and fibrinopeptide A release in man. *Journal of Laboratory and Clinical Medicine*, **69**, 592-604.

27 Lluis, F., Roma, J., Suelves, M., Parra, M., Aniorte, G., Gallardo, E., Illa, I., Rodriguez, L., Hughes, S.M., Carmeliet, P. *et al.* (2001) Urokinase-dependent plasminogen activation is required for efficient skeletal muscle regeneration in vivo. *Blood*, **97**, 1703-1711.

28 McRitchie, D.I., Girotti, M.J., Glynn, M.F., Goldberg, J.M. and Rotstein, O.D. (1991) Effect of systemic fibrinogen depletion on intraabdominal abscess formation. *J Lab Clin Med*, **118**, 48-55.

29 Tang, L. and Eaton, J.W. (1993) Fibrin(ogen) mediates acute inflammatory responses to biomaterials. *J Exp Med*, **178**, 2147-2156.

30 Akassoglou, K., Adams, R.A., Bauer, J., Mercado, P., Tseveleki, V., Lassmann, H., Probert, L. and Strickland, S. (2004) Fibrin depletion decreases inflammation and delays the onset of demyelination in a tumor necrosis factor transgenic mouse model for multiple sclerosis. *Proc Natl Acad Sci U S A*, **101**, 6698-6703.

31 Idell, S. (2003) Coagulation, fibrinolysis, and fibrin deposition in acute lung injury. *Crit Care Med*, **31**, S213-220.

32 Serrano, A.L. and Munoz-Canoves, P. (2010) Regulation and dysregulation of fibrosis in skeletal muscle. *Exp Cell Res*, **316**, 3050-3058.

33 Flick, M.J., Du, X., Witte, D.P., Jirouskova, M., Soloviev, D.A., Busuttil, S.J., Plow, E.F. and Degen, J.L. (2004) Leukocyte engagement of fibrin(ogen) via the integrin receptor alphaMbeta2/Mac-1 is critical for host inflammatory response in vivo. *J Clin Invest*, **113**, 1596-1606.

34 Adams, R.A., Bauer, J., Flick, M.J., Sikorski, S.L., Nuriel, T., Lassmann, H., Degen, J.L. and Akassoglou, K. (2007) The fibrin-derived gamma377-395 peptide inhibits microglia activation and suppresses relapsing paralysis in central nervous system autoimmune disease. *J Exp Med*, **204**, 571-582.

35 Flick, M.J., LaJeunesse, C.M., Talmage, K.E., Witte, D.P., Palumbo, J.S., Pinkerton, M.D., Thornton, S. and Degen, J.L. (2007) Fibrin(ogen) exacerbates inflammatory joint disease through a mechanism linked to the integrin alphaMbeta2 binding motif. *J Clin Invest*, **117**, 3224-3235.

36 Steinbrecher, K.A., Horowitz, N.A., Blevins, E.A., Barney, K.A., Shaw, M.A., Harmel-Laws, E., Finkelman, F.D., Flick, M.J., Pinkerton, M.D., Talmage, K.E. *et al.* (2010) Colitis-associated cancer is dependent on the interplay between the hemostatic and inflammatory systems and supported by integrin alpha(M)beta(2) engagement of fibrinogen. *Cancer Res*, **70**, 2634-2643.

37 Ugarova, T.P., Solovjov, D.A., Zhang, L., Loukinov, D.I., Yee, V.C., Medved, L.V. and Plow, E.F. (1998) Identification of a novel recognition sequence for integrin alphaM beta2 within the gamma-chain of fibrinogen. *J Biol Chem*, **273**, 22519-22527.

38 Ugarova, T.P. and Yakubenko, V.P. (2001) Recognition of fibrinogen by leukocyte integrins. *Ann N Y Acad Sci*, **936**, 368-385.

39 Sitrin, R.G., Pan, P.M., Srikanth, S. and Todd, R.F., 3rd (1998) Fibrinogen activates NF-kappa B transcription factors in mononuclear phagocytes. *J Immunol*, **161**, 1462-1470.

40 Rubel, C., Gomez, S., Fernandez, G.C., Isturiz, M.A., Caamano, J. and Palermo, M.S. (2003) Fibrinogen-CD11b/CD18 interaction activates the NF-kappa B pathway and delays apoptosis in human neutrophils. *Eur J Immunol*, **33**, 1429-1438.

41 Dhawan, J. and Rando, T.A. (2005) Stem cells in postnatal myogenesis: molecular mechanisms of satellite cell quiescence, activation and replenishment. *Trends Cell Biol*, **15**, 666-673.

42 Sanes, J.R. (2003) The basement membrane/basal lamina of skeletal muscle. *J Biol Chem*, **278**, 12601-12604.

43 Sinanan, A.C., Machell, J.R., Wynne-Hughes, G.T., Hunt, N.P. and Lewis, M.P. (2008) Alpha v beta 3 and alpha v beta 5 integrins and their role in muscle precursor cell adhesion. *Biol Cell*, **100**, 465-477.

44 Lygoe, K.A., Norman, J.T., Marshall, J.F. and Lewis, M.P. (2004) AlphaV integrins play an important role in myofibroblast differentiation. *Wound Repair Regen*, **12**, 461-470.

45 Liu, H., Niu, A., Chen, S.E. and Li, Y.P. (2011) Beta3-integrin mediates satellite cell differentiation in regenerating mouse muscle. *FASEB J*, **25**, 1914-1921.

46 Pizza, F.X., Peterson, J.M., Baas, J.H. and Koh, T.J. (2005) Neutrophils contribute to muscle injury and impair its resolution after lengthening contractions in mice. *J Physiol*, **562**, 899-913.

47 Pizza, F.X., McLoughlin, T.J., McGregor, S.J., Calomeni, E.P. and Gunning, W.T. (2001) Neutrophils injure cultured skeletal myotubes. *Am J Physiol Cell Physiol*, **281**, C335-341.

48 Spencer, M.J., Montecino-Rodriguez, E., Dorshkind, K. and Tidball, J.G. (2001) Helper (CD4(+)) and cytotoxic (CD8(+)) T cells promote the pathology of dystrophin-deficient muscle. *Clin Immunol*, **98**, 235-243.

49 Hodgetts, S., Radley, H., Davies, M. and Grounds, M.D. (2006) Reduced necrosis of dystrophic muscle by depletion of host neutrophils, or blocking TNFalpha function with Etanercept in mdx mice. *Neuromuscul Disord*, **16**, 591-602.

50 Flick, M.J., Du, X. and Degen, J.L. (2004) Fibrin(ogen)-alpha M beta 2 interactions regulate leukocyte function and innate immunity in vivo. *Exp Biol Med (Maywood)*, **229**, 1105-1110.

51 Nguyen, H.X. and Tidball, J.G. (2003) Interactions between neutrophils and macrophages promote macrophage killing of rat muscle cells in vitro. *J Physiol*, **547**, 125-132.

52 Cheung, E.V. and Tidball, J.G. (2003) Administration of the non-steroidal anti-inflammatory drug ibuprofen increases macrophage concentrations but reduces necrosis during modified muscle use. *Inflamm Res*, **52**, 170-176.

53 Pelosi, L., Giacinti, C., Nardis, C., Borsellino, G., Rizzuto, E., Nicoletti, C., Wannenes, F., Battistini, L., Rosenthal, N., Molinaro, M. *et al.* (2007) Local expression of IGF-1 accelerates muscle regeneration by rapidly modulating inflammatory cytokines and chemokines. *FASEB J*, **21**, 1393-1402.

54 Radley, H.G., Davies, M.J. and Grounds, M.D. (2008) Reduced muscle necrosis and long-term benefits in dystrophic mdx mice after cV1q (blockade of TNF) treatment. *Neuromuscul Disord*, **18**, 227-238.

55 Peterson, J.M. and Guttridge, D.C. (2008) Skeletal muscle diseases, inflammation, and NF-kappaB signaling: insights and opportunities for therapeutic intervention. *Int Rev Immunol*, **27**, 375-387.

56 Ahn, H.J., Zamolodchikov, D., Cortes-Canteli, M., Norris, E.H., Glickman, J.F. and Strickland, S. (2010) Alzheimer's disease peptide beta-amyloid interacts with fibrinogen and induces its oligomerization. *Proc Natl Acad Sci U S A*, **107**, 21812-21817.

57 Cortes-Canteli, M., Paul, J., Norris, E.H., Bronstein, R., Ahn, H.J., Zamolodchikov, D., Bhuvanendran, S., Fenz, K.M. and Strickland, S. (2010) Fibrinogen and beta-amyloid association alters thrombosis and fibrinolysis: a possible contributing factor to Alzheimer's disease. *Neuron*, **66**, 695-709.

58 Suh, T.T., Holmback, K., Jensen, N.J., Daugherty, C.C., Small, K., Simon, D.I., Potter, S. and Degen, J.L. (1995) Resolution of spontaneous bleeding events but failure of pregnancy in fibrinogen-deficient mice. *Genes & development*, **9**, 2020-2033.

59 Hamer, P.W., McGeachie, J.M., Davies, M.J. and Grounds, M.D. (2002) Evans Blue Dye as an in vivo marker of myofibre damage: optimising parameters for detecting initial myofibre membrane permeability. *J Anat*, **200**, 69-79.

60 Suelves, M., Lopez-Alemany, R., Lluis, F., Aniorte, G., Serrano, E., Parra, M., Carmeliet, P. and Munoz-Canoves, P. (2002) Plasmin activity is required for myogenesis in vitro and skeletal muscle regeneration in vivo. *Blood*, **99**, 2835-2844.

61 Celada, A., Gray, P.W., Rinderknecht, E. and Schreiber, R.D. (1984) Evidence for a gamma-interferon receptor that regulates macrophage tumoricidal activity. *J Exp Med*, **160**, 55-74.

62 Ugarova, T.P., Lishko, V.K., Podolnikova, N.P., Okumura, N., Merkulov, S.M., Yakubenko, V.P., Yee, V.C., Lord, S.T. and Haas, T.A. (2003) Sequence gamma 377-395(P2), but not gamma 190-202(P1), is the binding site for the alpha MI-domain of integrin alpha M beta 2 in the gamma C-domain of fibrinogen. *Biochemistry*, **42**, 9365-9373.

63 Perdiguero, E., Ruiz-Bonilla, V., Gresh, L., Hui, L., Ballestar, E., Sousa-Victor, P., Baeza-Raja, B., Jardi, M., Bosch-Comas, A., Esteller, M. *et al.* (2007) Genetic analysis of p38 MAP kinases in myogenesis: fundamental role of p38alpha in abrogating myoblast proliferation. *The EMBO journal*, **7**, 1245-1256.

FIGURE LEGENDS

Figure 1. Fibrin(ogen) accumulates in mdx dystrophic muscle, and fibrin(ogen) deficiency results in reduced muscle degeneration and enhanced regeneration. A. Fibrin(ogen) deposition was analyzed by immunohistochemistry in gastrocnemius muscles of WT control mice and in mdx mice of 14, 30 and 90 days of age. Magnification bar: 50 µm. **B.** Immunostaining for fibrin(ogen) of gastrocnemius muscles of 90-day-old mice showing the absence of fibrin(ogen) deposition in $Fib^{-/-}$mdx mice as compared to $Fib^{+/+}$mdx mice. Bar: 25 µm. **C.** Left: Reduced percentage of total muscle degeneration area in $Fib^{-/-}$mdx versus $Fib^{+/+}$mdx mice at 30 days of age, as determined by morphometric analysis on H&E stained gastrocnemius muscle sections. Right: Reduced muscle membrane damage in $Fib^{-/-}$mdx versus $Fib^{+/+}$mdx, as indicated by serum creatine kinase (CK) measurement. Data are mean ± S.E.M.; n= 5 animals per group (*, P<0.05, Mann Whitney Test). **D.** Increased cross-sectional area (CSA) of growing central-nucleated fibers (CNFs) in muscles of $Fib^{-/-}$ mdx mice as compared to $Fib^{+/+}$mdx mice (mean ± S.E.M., 566.5 ± 5.0 versus 394.5 ± 6.7 μm^2; n= 4 animals per group; P<0.001 Mann Whitney test); size frequency distribution of regenerating myofibers is represented. **E.** Reduced inflammatory infiltration in $Fib^{-/-}$mdx muscle. Top: localization of $\alpha_M\beta_2$ (CD11b/CD18 or Mac-1) positive macrophages in the damaged areas of mdx muscle occupied by fibrin(ogen) is shown by immunofluorescence. Bar: 25 µm. Bottom left: quantification of F4/80 positive cells by flow cytometry analysis. Data are mean ± S.E.M.; n= 3 animals per group (*, P<0.05, Mann Whitney test). Bottom right: quantification of macrophages in $Fib^{-/-}$mdx versus $Fib^{+/+}$mdx muscles. Data are mean ± S.E.M.; n= 5 animals per group (*, P<0.05, Mann Whitney Test). **F**. Cardiotoxin (CTX)-injury in muscle of $Fib^{-/-}$ and $Fib^{+/+}$ mice. Quantification of macrophage numbers at 3 days post-injury in degenerating areas showed reduced infiltration in $Fib^{-/-}$ mice. Data are mean ± S.E.M.; n= 5 animals per group (*, P<0.05, Mann Whitney Test). **G.** At 5 days post-injury, the CSA of growing CNFs was larger in $Fib^{-/-}$ mice than in $Fib^{+/+}$ controls; frequency distribution of myofiber size is represented (mean ± S.E.M., 141.8 ± 1.9 versus 109.5 ± 1.3 μm^2; 4 animals per group; P<0.001 Mann Whitney test).

Figure 2. Pharmacological defibrination attenuates dystrophy progression in mdx muscle. 12 day-old mdx mice were subjected to a defibrination treatment by daily intraperitoneal injection with ancrod (or with vehicle – control saline solution), up to 2.5 months of age. **A.** Fibrin(ogen) staining of muscle sections of vehicle-treated and defibrinated mdx mice. Bar: 50 µm. **B.** Left: Percentage of total muscle degeneration area**.** Right: Muscle membrane damage indicated by serum CK levels. Data are mean ± S.E.M.; n= 5 animals per group (*, P<0.05). **C.** Frequency distribution of regenerating myofiber size. (mean ± S.E.M., 576.4 ± 11.5 mdx defibrinated versus 471.6 ± 12.1 μm^2 mdx vehicle; 6 animals per group; P<0.001 Mann Whitney test) **D.** Increased functional muscle strength in defibrinated versus vehicle-treated mdx mice. Left: Four limb grip strength. Right: Distance to reach exhaustion in treadmill

assays. Data are mean ± S.E.M.; 5 animals per group; (*, P<0.05 versus mdx vehicle, Mann Whitney test).

Figure 3. Intramuscular delivery of fibrinogen induces a tissue injury/repair-like response in fibrinogen null mice.

A. Fibrin(ogen) and $\alpha_M\beta_2$ co-immunostaining of muscle sections of non-injured WT mice and at 2, 4 and 12 hours after CTX injury. Bar: 25 µm. **B.** 2-month-old $Fib^{-/-}$ mice were subjected to intramuscular delivery of saline (vehicle) or fibrinogen (9 mg/ml) into the right and left tibialis muscles, respectively. Left: Representative pictures of saline and fibrinogen injected muscles stained for fibronectin and $\alpha_M\beta_2$. Bar: 25 µm. Right: Quantification of the number of macrophages showed increased infiltration in fibrinogen- versus saline-treated muscles in $Fib^{-/-}$ mice at day 3 after injection. Data are mean ± S.E.M.; n= 4 animals per group; (*, $P<0.05$ versus saline treated animals, Mann Whitney test). **C.** Induction of muscle degeneration and regeneration by fibrinogen delivery in $Fib^{-/-}$ mice. Left: Percentages of total muscle degeneration area in saline versus fibrinogen -treated $Fib^{-/-}$ muscle at 2 days after injury, as determined by morphometric analysis on H&E stained sections. Data are mean ± S.E.M.; n= 4 animals per group; (*, $P<0.05$ versus $Fib^{-/-}$ saline, Mann Whitney test). Right: Presence of numerous eMHC positive fibers at 5 days after fibrinogen administration to $Fib^{-/-}$ muscles as revealed by immunoperoxidase staining. Bar: 25 µm.

Figure 4. Interaction of fibrin(ogen) with $\alpha_M\beta_2$ integrin receptor on macrophages regulates inflammation, degeneration and regeneration in mdx muscle.

A. Representative macrophage F4/80 immunostaining of muscle sections from $Fib^{+/+}$mdx and $Fib\gamma^{390-396A}$mdx mice. Bar: 50 µm. **B.** Reduced muscle inflammatory macrophage infiltration analyzed by flow cytometry (*, $p<0.05$ versus $Fib^{+/+}$mdx animals, Mann Whitney Test, n=3 animals per group) and morphologically by immunohistochemistry, percentage of total muscle degeneration area in gastrocnemius muscles and serum CK levels in 2.5 month-old $Fib\gamma^{390-396A}$mdx mice as compared with age-matched $Fib^{+/+}$mdx mice. Data are mean ± S.E.M.; n= 4 animals per group; (*, $p<0.05$ versus $Fib^{+/+}$mdx animals, Mann Whitney Test). **C.** Increased CSA of growing CFNs in $Fib\gamma^{390-396A}$mdx versus $Fib^{+/+}$mdx muscle. Frequency distribution of regenerating myofiber size is represented. (mean ± S.E.M., 576.3 ± 7.4 $Fib\gamma^{390-396A}$mdx versus 481.4 ± 7.5 μm^2 $Fib^{+/+}$mdx; 4 animals per group; $P<0.001$ Mann Whitney test). **D.** Increased performance in $Fib\gamma^{390-396A}$mdx versus $Fib^{+/+}$mdx mice of 2.5 months of age, using four limb grip strength assays and treadmill exhaustion test. Data are mean ± SEM; n= 5 animals per group. (*, $P<0.05$ versus $Fib^{+/+}$mdx, Mann Whitney Test). **E.** Quantification of the number of macrophages (identified by F4/80 immunostaining) 3 days after CTX injury showing reduced inflammation in muscles of $Fib\gamma^{390-396A}$ mice. Data are mean ± SEM; n= 4 animals per group; (*, $P<0.05$, Mann Whitney Test). **F.** CTX-injured $Fib\gamma^{390-396A}$ mice show enhanced growth of regenerating myofibers compared with WT counterparts at day 5 after injury. Fiber size distribution is shown. (mean ± S.E.M., 148.2 ± 1.4 $Fib\gamma^{390-396A}$ versus 120.6 ± 1.4 μm^2 $Fib^{+/+}$; 4 animals per group; $P<0.001$ Mann Whitney test).

Figure 5. Treatment with a fibrinogen-derived $\gamma^{377-395}$ peptide blocks inflammation and disease progression in mdx mice.

A. Activation of macrophages by fibrin(ogen) is reduced by the fibrinogen-γ-derived 377-395 peptide. Primary macrophages were treated with fibrinogen (Fg) in the absence or presence of the $\gamma^{377-395}$ peptide or scrambled peptide used as control. Additional experimental controls included treatment with an $\alpha_M\beta_2$ blocking antibody, or IgG control antibody, as indicated. Expression of inflammatory cytokines was analyzed by qRT-PCR. Results are fold-induction values with respect to untreated macrophages. Data are mean ± SEM; n= 3 experiments performed in triplicate; (*, P<0.05 versus control conditions, Mann Whitney Test) **B.** Inflammation is attenuated by treatment with the $\gamma^{377-395}$ peptide in mdx mice. Mdx mice of 2 months of age were treated with $\gamma^{377-395}$ peptide, or scrambled peptide as control, for the course of three weeks. Data are mean ± S.E.M.; n= 5 animals per group (*, P<0.05, Mann Whitney Test). **C.** Left: Percentage of total muscle degeneration area in mdx mice treated with $\gamma^{377-395}$ or scrambled peptides. Data are mean ± S.E.M.; n= 5 animals per group (*, P<0.05, Mann Whitney Test). Right: Extent of muscle membrane damage in mdx mice before and after the treatment with $\gamma^{377-395}$ peptide (or scrambled peptide) as indicated by serum CK levels. Data are mean ± S.E.M.; n= 5 animals per group (*, P<0.05 versus CK values of the same animals before the treatment, Mann Whitney Test) **D.** Frequency distribution of the size of regenerating myofibers in mdx mice treated with $\gamma^{377-395}$ peptide (or scrambled peptide), (mean ± S.E.M., 515.8 ± 8.4 mdx $\gamma^{377-395}$ peptide versus 440.5 ± 8.4 μm^2 mdx scrambled peptide; 4 animals per group; P<0.001 Mann Whitney test). **E.** Reduced cytokine expression in muscles of mdx mice treated with $\gamma^{377-395}$ peptide compared to scrambled peptide-treated mice by qRT-PCR analysis. Data are mean ± S.E.M.; n= 5 animals per group (*, P<0.05 versus scrambled peptide treatment, Mann Whitney Test) **F.** Left: Increased muscle grip strength of mdx mice treated with $\gamma^{377-395}$ peptide compared to scramble peptide-treated mice. Right: Improvement of treadmill performance in an exhaustion test of mdx mice treated with a $\gamma^{377-395}$ peptide. Data are mean ± SEM; n= 5 animals per group (*, P<0.05 versus values of the same group before the treatment, Mann Whitney Test).

Figure 6. Paracrine effect of fibrinogen-activated macrophages on satellite cells.

Satellite cells obtained from mouse muscle were cultured in growth medium (GM) for 24 hours with conditioned medium (CM) from macrophages treated or not with fibrinogen for 24 hours (CM Fg), and incubated for 1 hour with BrdU. When indicated, the $\gamma^{377-395}$ peptide or scramble peptide were added to fibrinogen-stimulated macrophages. Also, neutralizing antibodies against TNFα and IL-1β (or control IgG) were added to CM from fibrinogen-stimulated macrophages **A.** Satellite cells subjected to the different macrophage conditioned media were fixed and immunostained for BrdU, and positive cells were quantified. **B.** Satellite cells were cultured in GM and then shifted to

differentiation medium, supplemented with different macrophage conditioned media as above. Comparative qRT-PCR analysis of Myogenin. **C.** eMHC mRNA expression. Results represent the mean of at least three experiments. Data are mean ± SEM; (*, P<0.05 versus control, One-way analysis of variance and Dunnett's multiple comparison test).

Figure 7. Fibrin(ogen) directly affects satellite cell functions.

A. Fibrin(ogen) is deposited in the basal laminae of dystrophic muscle. Top: Representative example of a double immunofluorescence staining showing an activated satellite cell in green (MyoD positive, see arrow) surrounded by fibrin(ogen) (red) in a 2.5 month old mdx gastrocnemius muscle section. Nuclei were stained with DAPI. Magnification bars: 10 μm. Bottom: Immunohistochemistry showing fibrin(ogen) (red) and laminin (green) co-staining in a mdx muscle section. Bar: 25 μm. **B.** Fibrinogen alters satellite cell functions. Left: Satellite cells were cultured in GM with and without increasing amounts of fibrinogen (500 and 1,000 μg Fibrinogen), and viable cells were counted after 72 h as an index of cell division. Data are mean ± SEM; n= 3 experiments performed in triplicate; (*, P<0.05 versus control conditions, One-way analysis of variance and Dunnett's multiple comparison test) Right: Satellite cells were cultured in GM in the absence or presence of 500 μg of fibrinogen, and incubated for 1 hour with BrdU. When indicated, an RGD peptide (a cyclic peptide that specifically interferes with αvβ3 integrin binding to ligand RGD motif) or non-specific RGD control (n.s. RGD) was also used to demonstrate fibrinogen-integrin effects on satellite cell proliferation. Similarly, a neutralizing antibody against αv integrin (or control IgG) was added. Proliferation rates were expressed as percentage of BrdU-positive cells relative to control. Data are mean ± SEM; n= 3 experiments performed in triplicate; (*, P<0.05 versus control conditions, One-way analysis of variance and Dunnett's multiple comparison test) **C.** Satellite cells cultured in GM were switched to DM to induce fusion. After 48h, cells were immunostained for eMHC to define nuclei inside myotubes and fusion rates were calculated. Data are mean ± SEM; n= 3 experiments performed in triplicate; (*, P<0.05 versus control matrigel conditions, Mann Whitney Test)

Figure 8. Association of fibrin(ogen) deposits and macrophage infiltrates in dystrophic muscle of DMD patients.

A. Representative examples of fibrin(ogen) accumulation and $\alpha_M\beta_2$ co-staining in sections of muscle biopsies from DMD patients compared to healthy individuals. Scale bar: 25 μm. **B.** Proposed model for the deleterious action of persistently deposited fibrin(ogen) in the dystrophic muscle ECM, after extravasation. Exacerbated deposition of fibrin(ogen) promotes inflammation-mediated muscle degeneration and regeneration via $\alpha_M\beta_2$ integrin engagement on macrophages thus inducing expression of pro-inflammatory cytokines, which in turn may negatively regulate

satellite cell functions. Fibrin(ogen) may also directly impact on satellite cells functions through $\alpha_V\beta_3$ integrin binding.

Figure S1. Reduced muscle membrane permeability in fibers from mdx muscles in the absence of fibrinogen. A. Representative pictures of serial cryosections of gastrocnemius muscles obtained from control WT, $Fib^{+/+}$mdx and $Fib^{-/-}$mdx mice injected with Evans Blue Dye as marker of myofiber permeability (59). Hematoxylin/eosin staining (H&E; bright field) and direct red fluorescence pictures of the dye-labeled damaged fibers is shown. Arrows mark the same fibers on serial sections. Note the absence of red fluorescence in undamaged control WT muscles. Scale bar: 100 µm.

Figure S2. Fibrin(ogen) extravasation promotes inflammation in mdx muscle. A. Top: Representative H&E pictures of the three different areas analyzed (see below) in gastrocnemius muscles of mdx mice of 2.5 months of age. Bar: 25 µm. Bottom: Fibrin(ogen) immunostaining of the same type of morphologically distinguishable areas. Bar: 50 µm **B.** Left: quantification of F4/80 positive cells by flow cytometry analisis. Data are mean ± S.E.M.; n= 3 animals per group (*, $P<0.05$, Mann Whitney test). Middle: Cell counts for macrophages detected by immunohistochemistry using anti-F4/80 antibody. Right: Macrophage counts at different stages of the degeneration/regeneration cycle. Three distinct consecutive phases were analyzed: I. Areas with extensive degeneration, persistence of necrotic fibers and absence of regenerating myofibers. II. Areas of very small nascent myofibers and absence of necrotic fibers. III. Areas of early myofiber regeneration containing well-defined, small regenerating myofibers and bigger than ones in stage II. Data are mean ± S.E.M.; n= 5 animals per group; (*, $P<0.05$ versus mdx vehicle, Mann Whitney test). **C.** Gene expression analysis by qRT-PCR in gastrocnemius muscles of 2.5 month-old mdx mice, treated with ancrod or vehicle for 2 months. Results are expressed as fold induction over expression level in age-matched WT mice. Data are mean ± S.E.M.; n= 4 animals per group; (*, $P<0.05$ versus mdx vehicle, Mann Whitney test). **D.** CTX injury in gastrocnemius muscles of WT mice treated with ancrod or vehicle, starting 12 h prior to CTX injection. Left: Number of macrophages per mm^2 of degenerating area at 3 days after CTX injury. Data are mean ± S.E.M.; n= 4 animals per group; (*, $P<0.05$ versus vehicle treated animals, Mann Whitney test). Right: CSA frequency distribution of regenerating myofibers at 5 days after CTX injury (mean ± S.E.M., 156.9 ± 2.1 defibrinated versus 122.8 ± 1.5 μm^2 vehicle; 5 animals per group; $P<0.001$ Mann Whitney test).

Figure S3. Association of fibrin(ogen) deposits and macrophage infiltrates in dystrophic muscle of DMD patients.

A. Higher magnification images as in Figure 8 A, showing the specificity of fibrin(ogen) accumulation and the presence of $\alpha_M\beta_2$ positive macrophages in biopsies of DMD patients. Scale

bar: 25 μm.

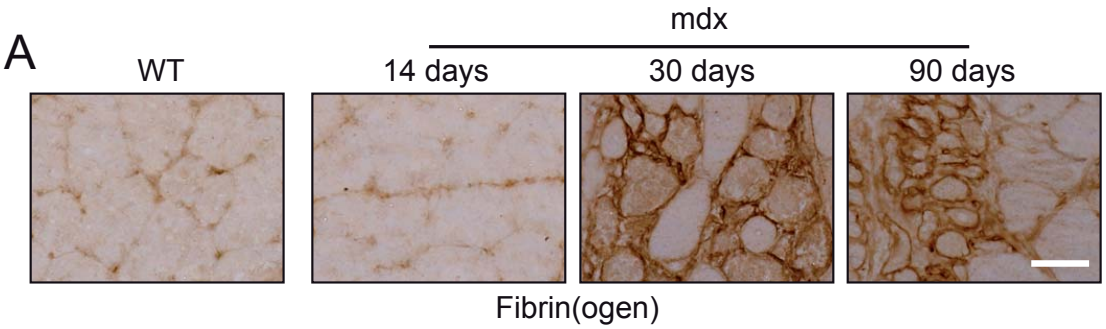
A
mdx
WT
14 days
30 days
90 days
Fibrin(ogen)

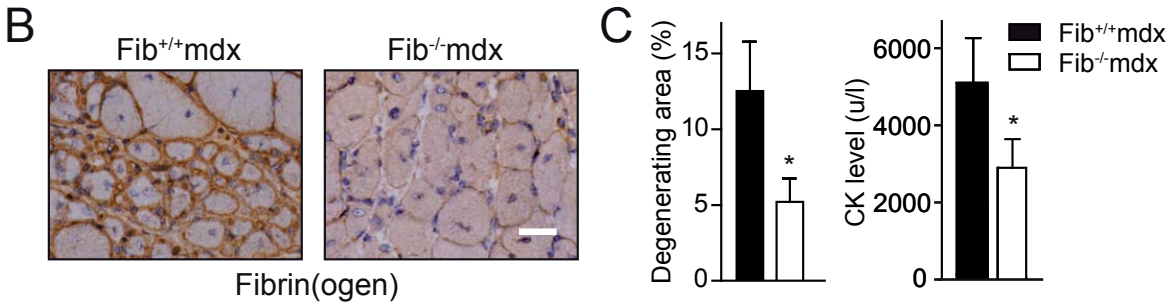
B
Fib+/+mdx
Fib-/-mdx
Fibrin(ogen)
C
Degenerating area (%)
CK level (u/l)
Fib+/+mdx
Fib-/-mdx

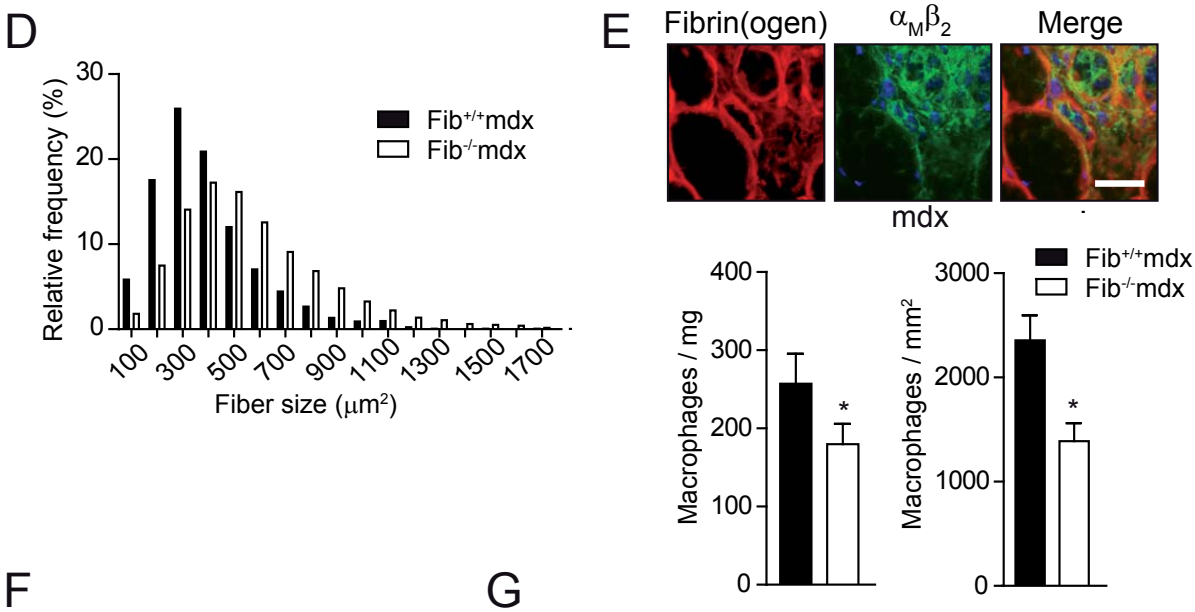
D
Relative frequency (%)
Fib+/+mdx
Fib-/-mdx
Fiber size (μm²)
E
Fibrin(ogen)
αMβ2
Merge
mdx
Macrophages / mg
Macrophages / mm²

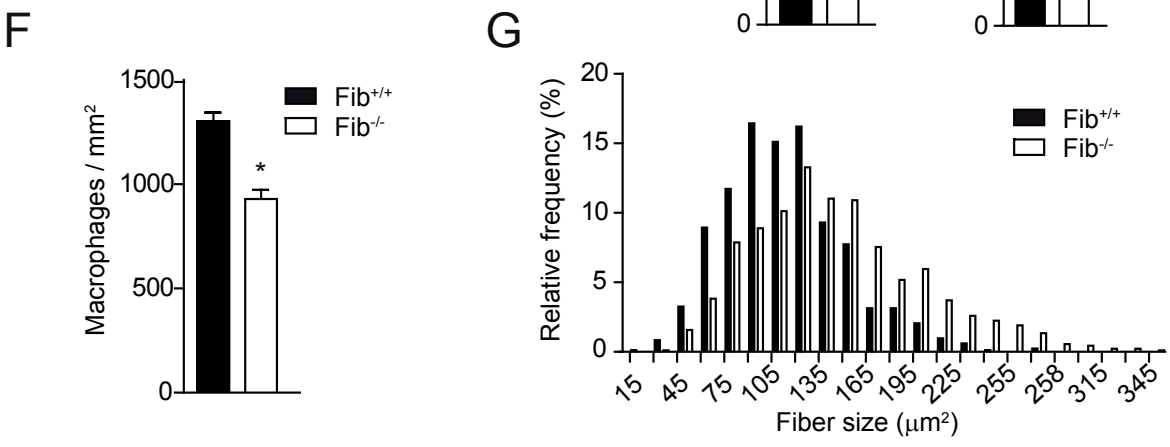
F
Macrophages / mm²
Fib+/+
Fib-/-
G
Relative frequency (%)
Fiber size (μm²)

Figure 1

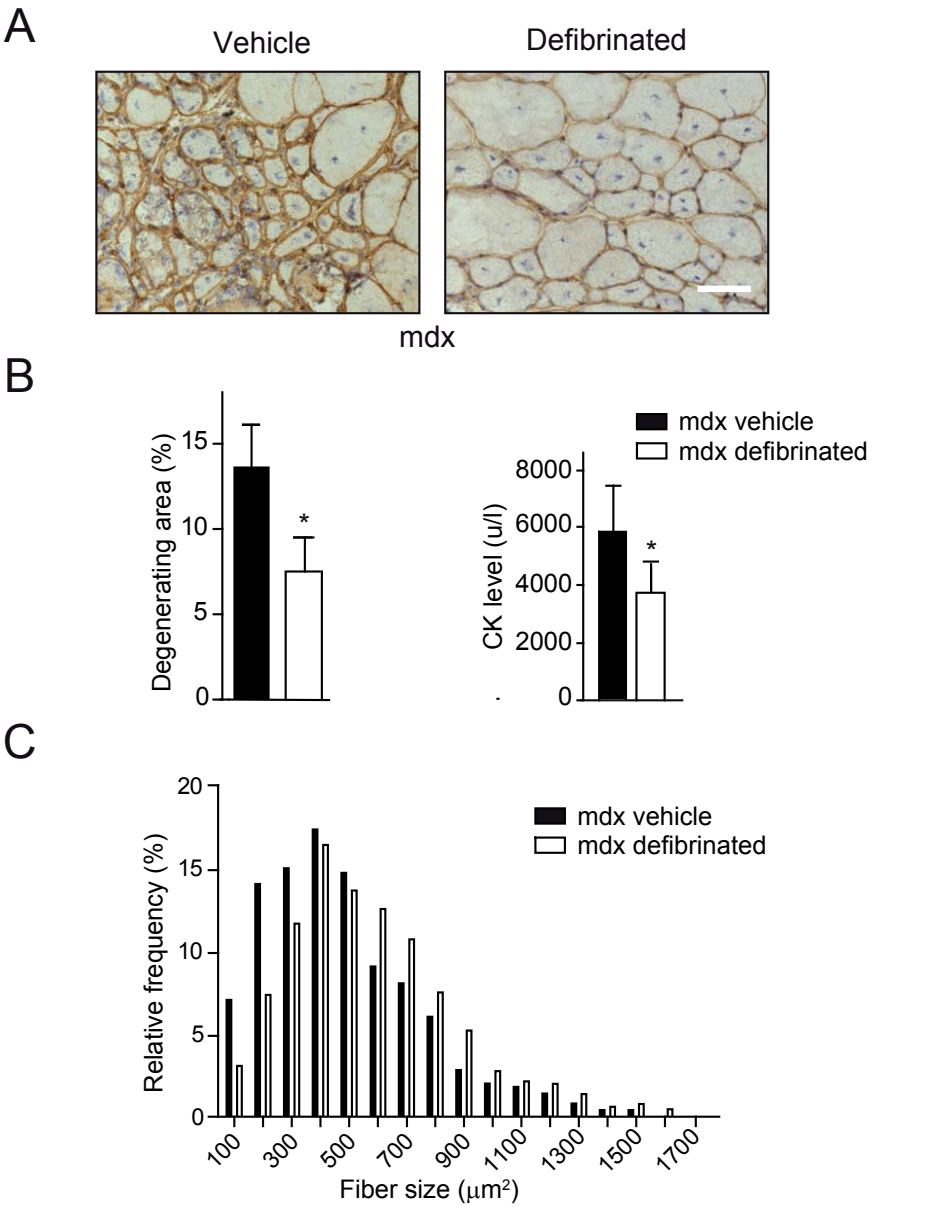
A
Vehicle
Defibrinated
mdx
B
Degenerating area (%)
0
5
10
15
*
CK level (u/l)
0
2000
4000
6000
8000
*
mdx vehicle
mdx defibrinated
C
Relative frequency (%)
0
5
10
15
20
100
300
500
700
900
1100
1300
1500
1700
Fiber size (μm²)
mdx vehicle
mdx defibrinated
D
Grip strength (g)
0
50
100
150
200
250
*
Distance to exahustion (m)
0
200
400
600
*
WT
mdx vehicle
mdx defibrinated

Figure 2

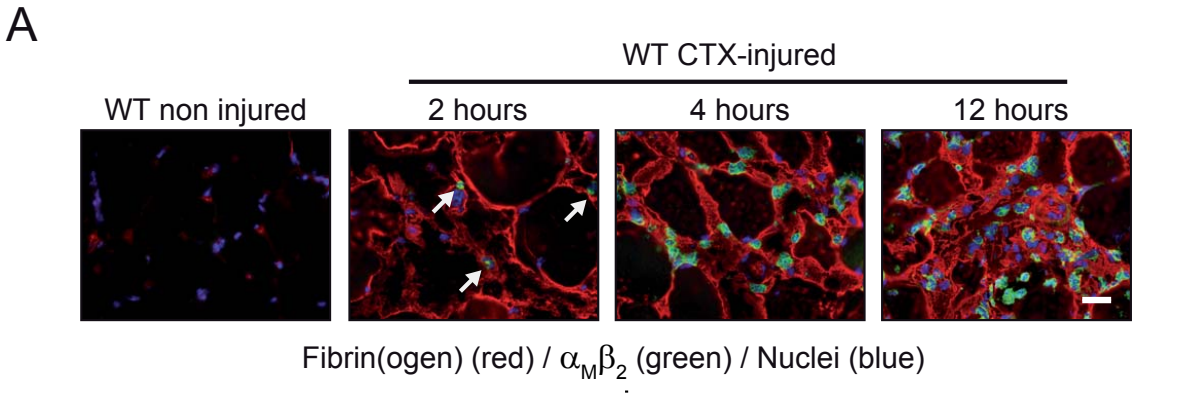
A
WT CTX-injured
WT non injured
2 hours
4 hours
12 hours
Fibrin(ogen) (red) / $\alpha_M\beta_2$ (green) / Nuclei (blue)

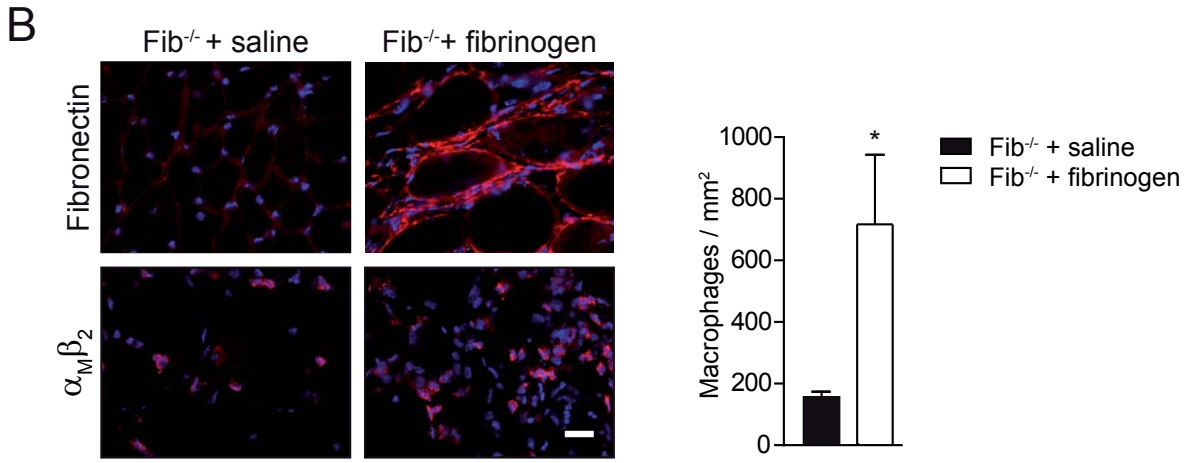
B
Fib-/- + saline
Fib-/-+ fibrinogen
Fibronectin
$\alpha_M\beta_2$
Macrophages / mm2
1000
800
600
400
200
0
*
Fib-/- + saline
Fib-/- + fibrinogen

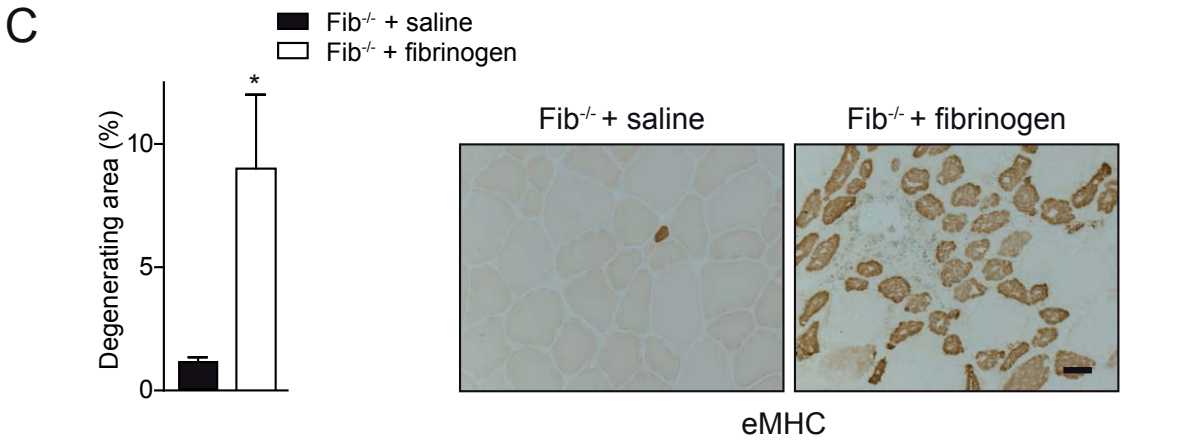
C
Fib-/- + saline
Fib-/- + fibrinogen
Degenerating area (%)
10
5
0
*
Fib-/- + saline
Fib-/- + fibrinogen
eMHC

Figure 3

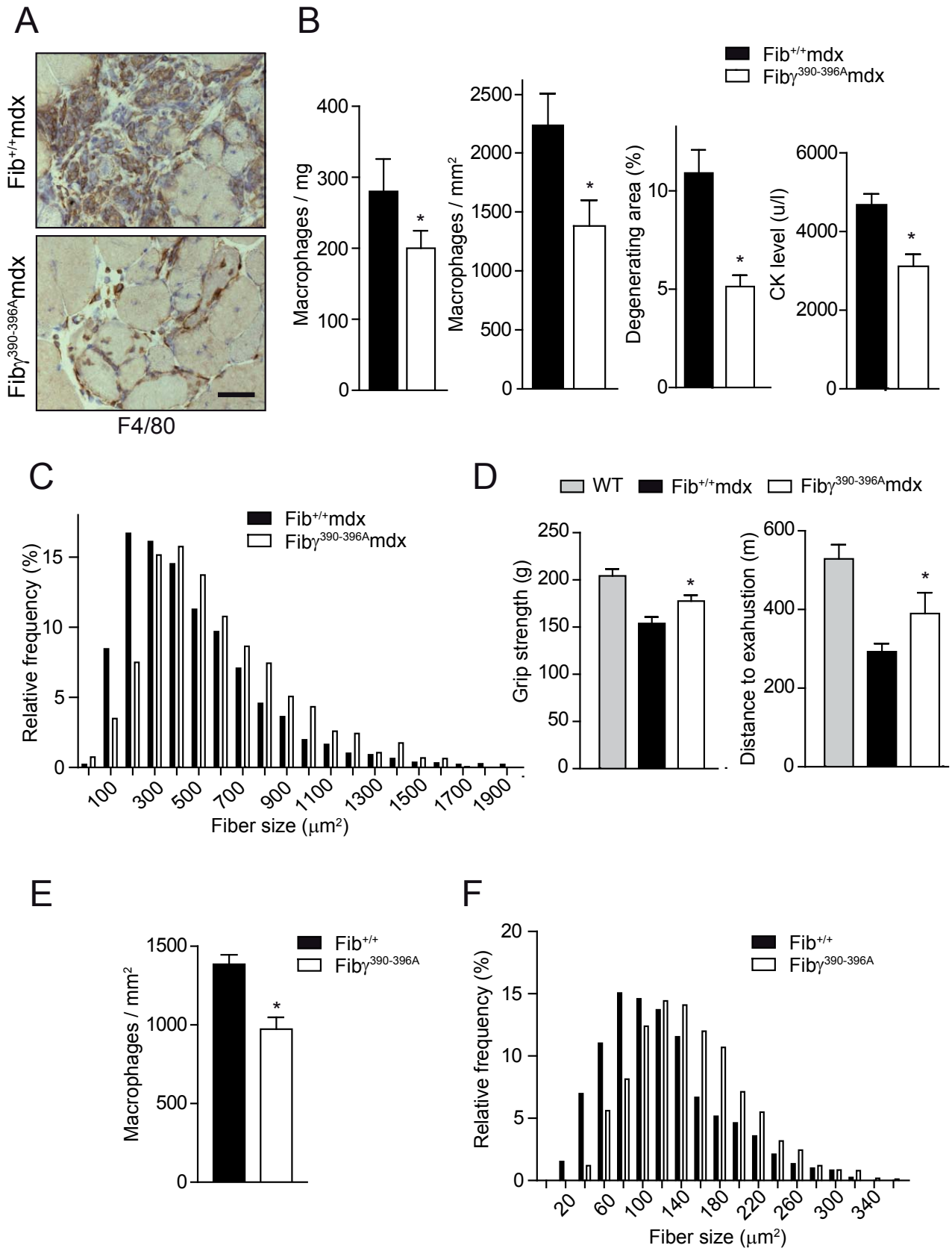
A
Fib+/+mdx
Fibγ390-396Amdx
F4/80
B
Fib+/+mdx
Fibγ390-396Amdx
Macrophages / mg
Macrophages / mm2
Degenerating area (%)
CK level (u/l)
C
Fib+/+mdx
Fibγ390-396Amdx
Relative frequency (%)
Fiber size (μm2)
D
WT
Fib+/+mdx
Fibγ390-396Amdx
Grip strength (g)
Distance to exahustion (m)
E
Fib+/+
Fibγ390-396A
Macrophages / mm2
F
Fib+/+
Fibγ390-396A
Relative frequency (%)
Fiber size (μm2)

Figure 4

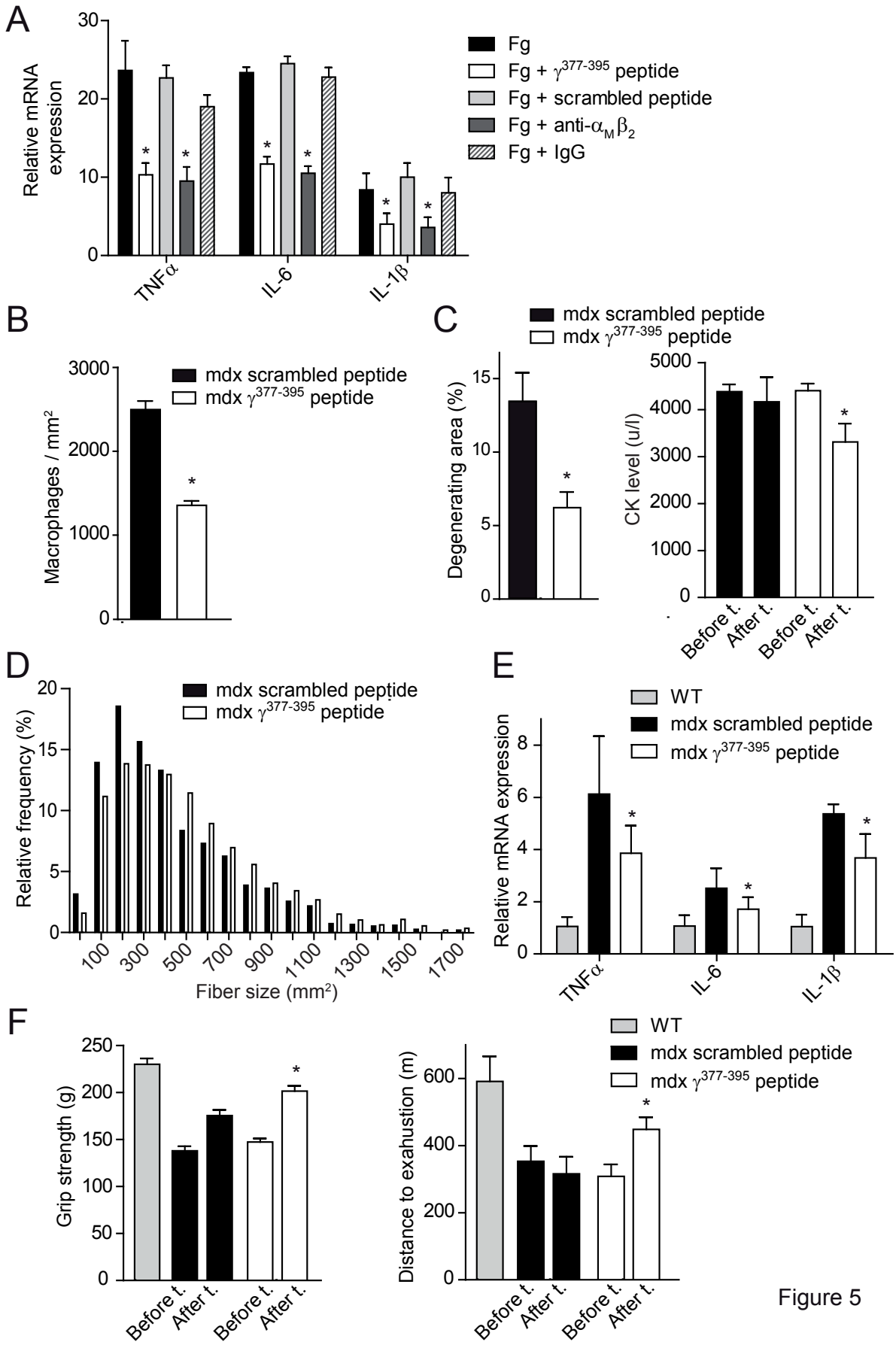
A
Relative mRNA expression
30
20
10
0
TNFα
IL-6
IL-1β
Fg
Fg + γ377-395 peptide
Fg + scrambled peptide
Fg + anti-αMβ2
Fg + IgG
B
Macrophages / mm2
3000
2000
1000
0
mdx scrambled peptide
mdx γ377-395 peptide
C
mdx scrambled peptide
mdx γ377-395 peptide
Degenerating area (%)
15
10
5
0
CK level (u/l)
5000
4000
3000
2000
1000
0
Before t.
After t.
Before t.
After t.
D
Relative frequency (%)
20
15
10
5
0
mdx scrambled peptide
mdx γ377-395 peptide
100
300
500
700
900
1100
1300
1500
1700
Fiber size (mm2)
E
WT
mdx scrambled peptide
mdx γ377-395 peptide
Relative mRNA expression
8
6
4
2
0
TNFα
IL-6
IL-1β
F
Grip strength (g)
250
200
150
100
50
0
Before t.
After t.
Before t.
After t.
WT
mdx scrambled peptide
mdx γ377-395 peptide
Distance to exahustion (m)
600
400
200
0
Before t.
After t.
Before t.
After t.

Figure 5

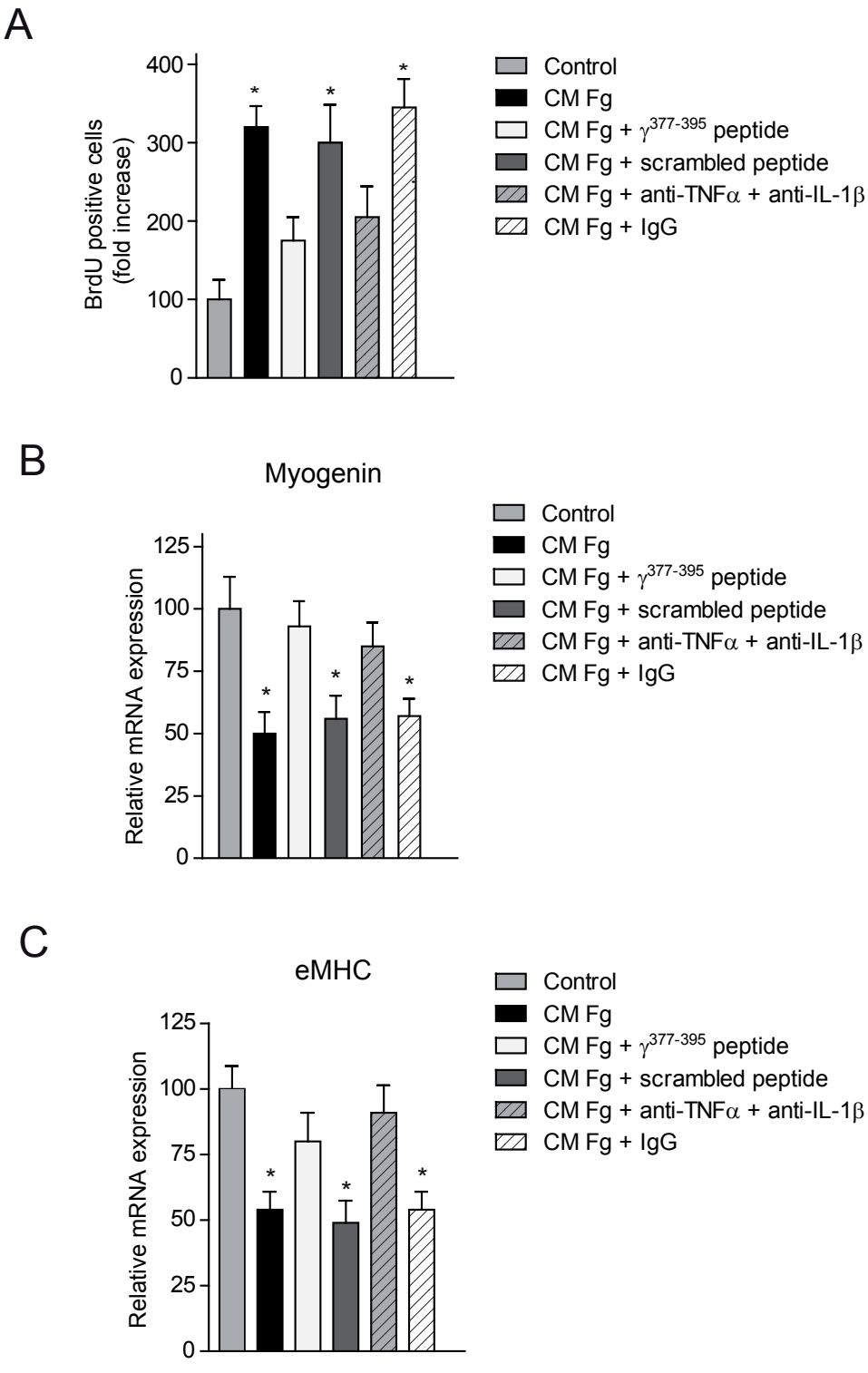
A
BrdU positive cells (fold increase)
400
300
200
100
0
*
Control
CM Fg
CM Fg + γ377-395 peptide
CM Fg + scrambled peptide
CM Fg + anti-TNFα + anti-IL-1β
CM Fg + IgG
B
Myogenin
Relative mRNA expression
125
100
75
50
25
0
C
eMHC

Figure 6

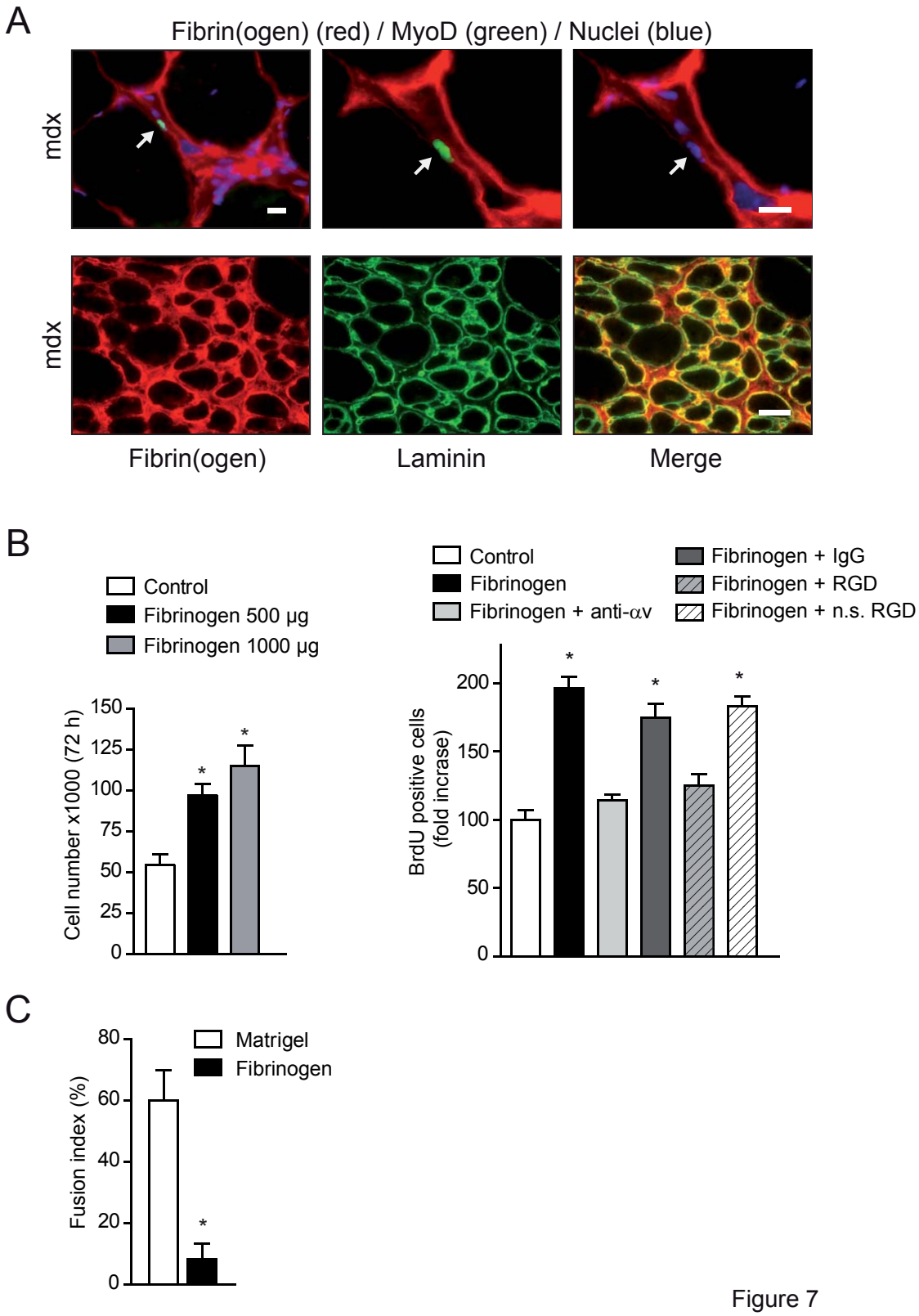
A
Fibrin(ogen) (red) / MyoD (green) / Nuclei (blue)
mdx
mdx
Fibrin(ogen)
Laminin
Merge
B
Control
Fibrinogen 500 µg
Fibrinogen 1000 µg
Cell number x1000 (72 h)
150
125
100
75
50
25
0
*
*
Control
Fibrinogen
Fibrinogen + anti-αv
Fibrinogen + IgG
Fibrinogen + RGD
Fibrinogen + n.s. RGD
BrdU positive cells
(fold incrase)
200
150
100
50
0
*
*
*
C
Matrigel
Fibrinogen
Fusion index (%)
80
60
40
20
0
*

Figure 7

A

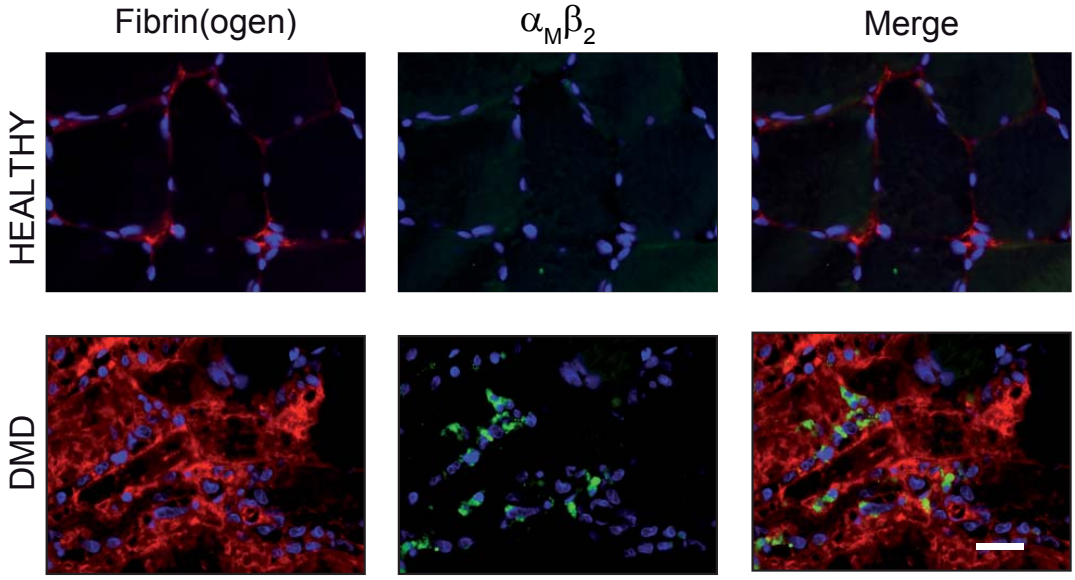
Fibrin(ogen)
$\alpha_M\beta_2$
Merge
HEALTHY
DMD

B

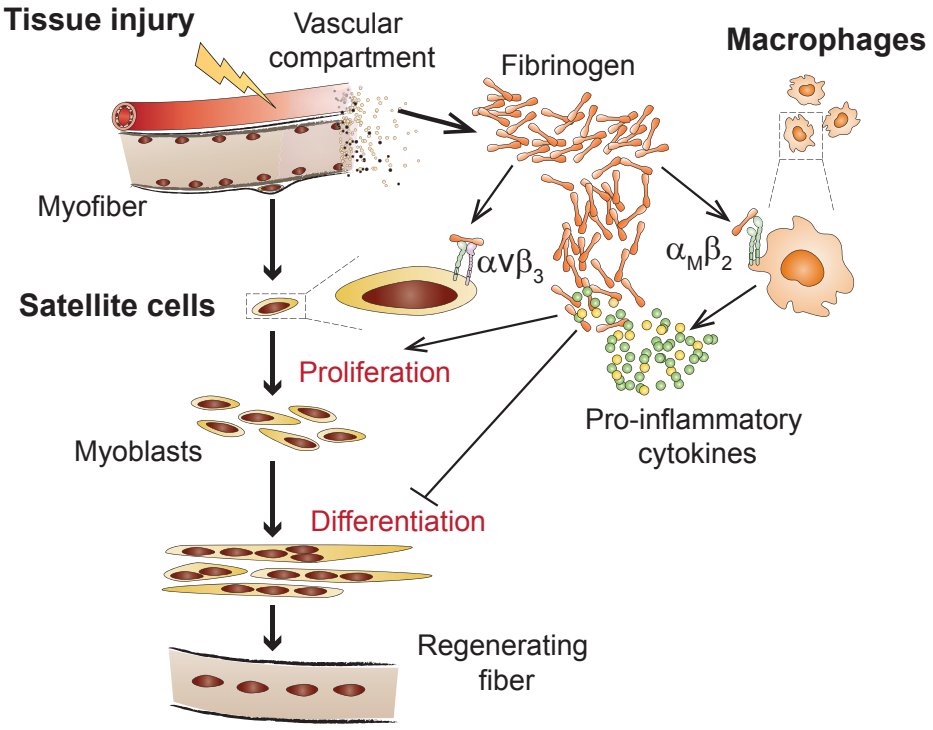
Tissue injury
Vascular compartment
Fibrinogen
Macrophages
Myofiber
$\alpha v\beta_3$
$\alpha_M\beta_2$
Satellite cells
Proliferation
Myoblasts
Pro-inflammatory cytokines
Differentiation
Regenerating fiber

Figure 8

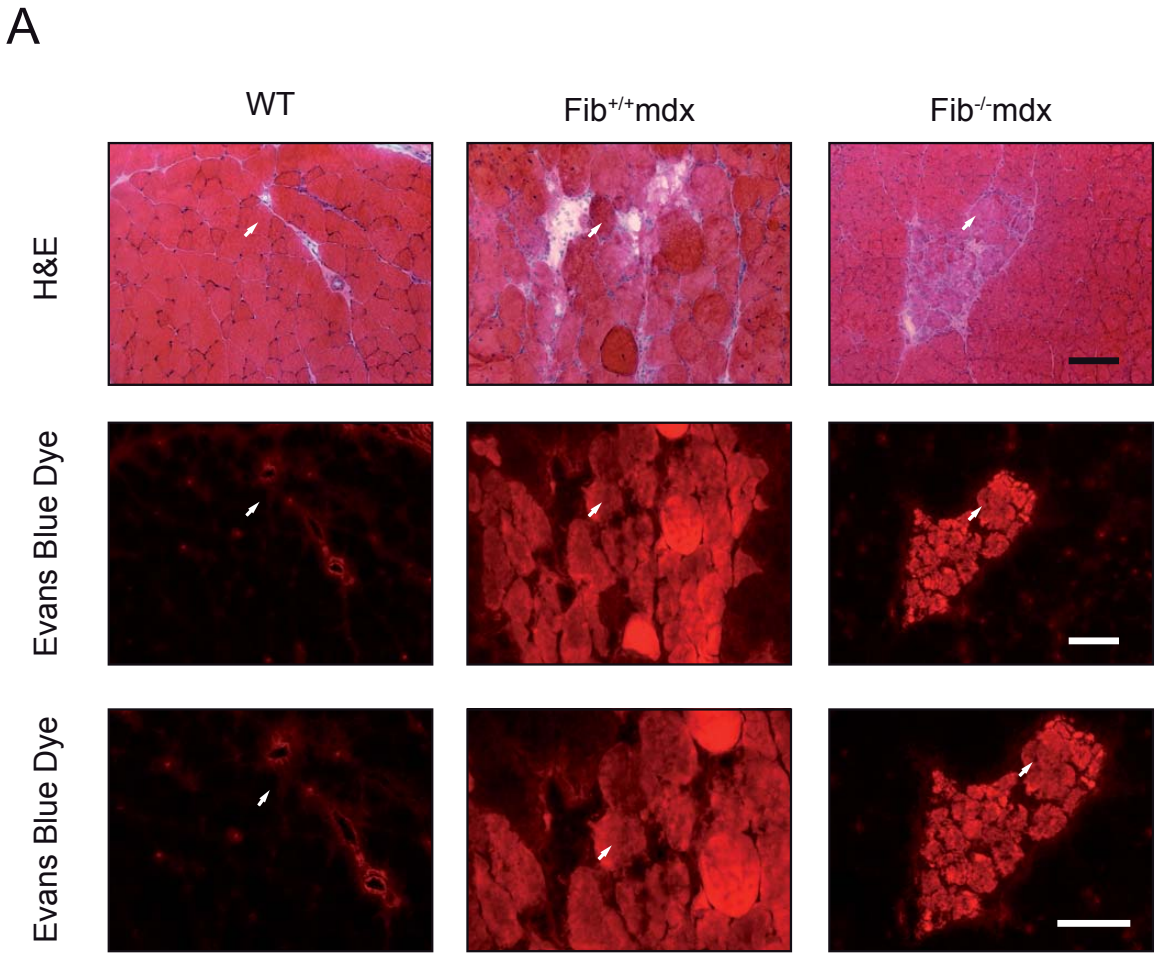

Figure S1

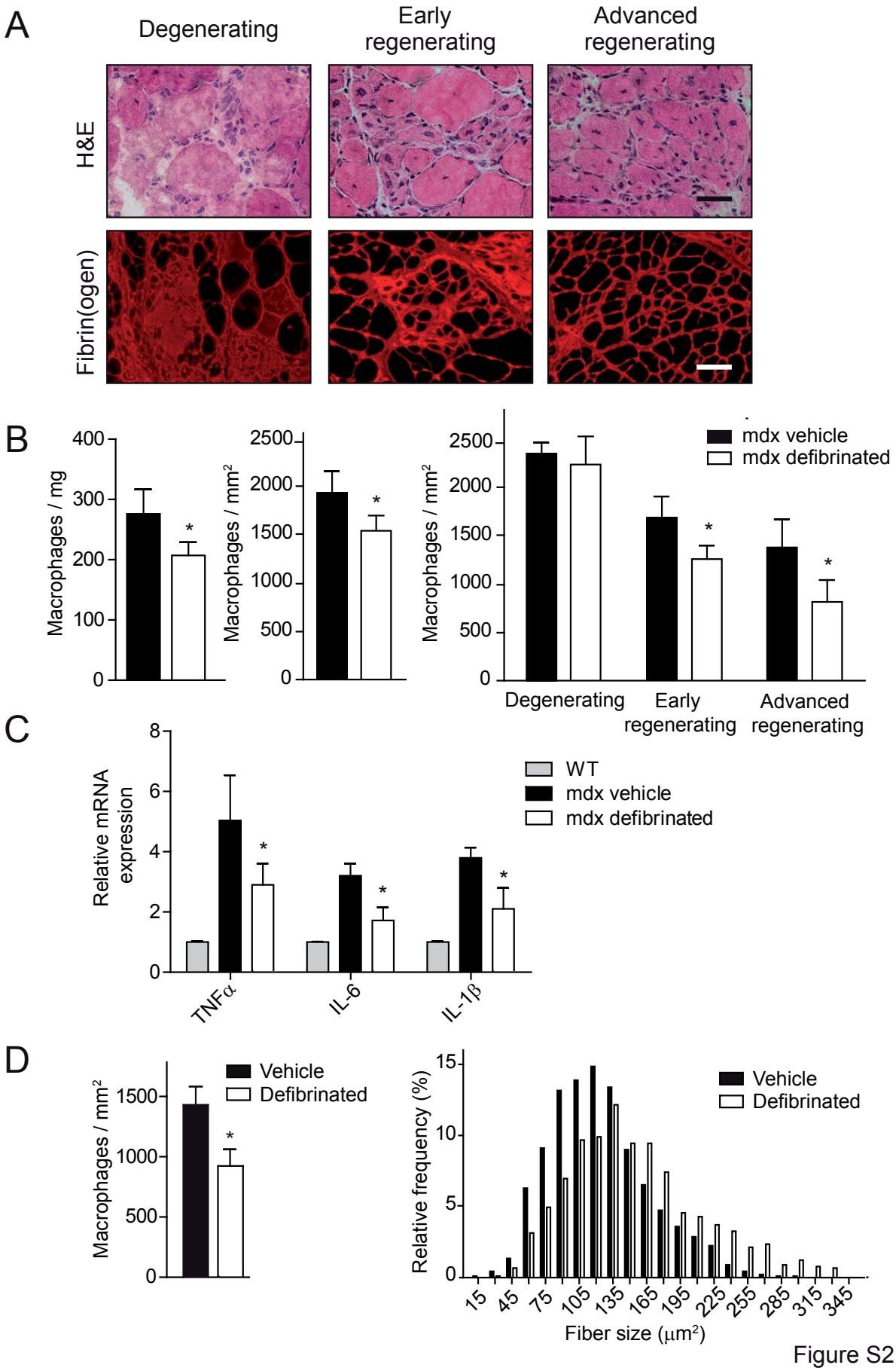
A
Degenerating
Early regenerating
Advanced regenerating
H&E
Fibrin(ogen)
B
Macrophages / mg
Macrophages / mm²
mdx vehicle
mdx defibrinated
Degenerating
Early regenerating
Advanced regenerating
C
Relative mRNA expression
WT
mdx vehicle
mdx defibrinated
TNFα
IL-6
IL-1β
D
Macrophages / mm²
Vehicle
Defibrinated
Relative frequency (%)
Fiber size (μm²)

Figure S2

A

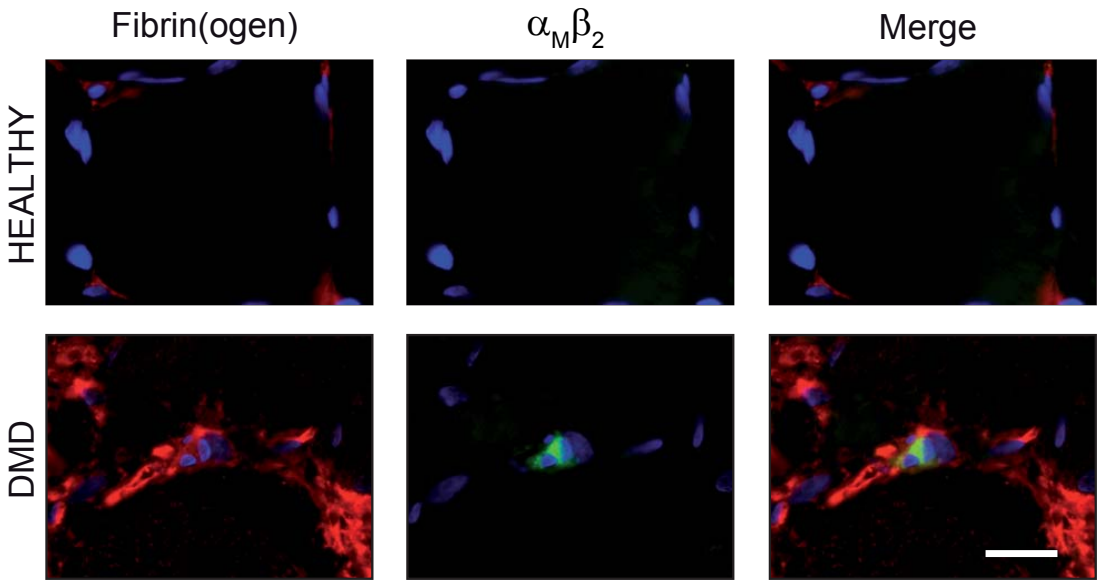

Figure S3